5-2017

Withaferin a synergistically enhances the effects of paclitaxel against lung cancer.

Al Hassan Kyakulaga
University of Louisville

WITHAFERIN A SYNERGISTICALLY ENHANCES THE EFFECT OF PACLITAXEL AGAINST LUNG CANCER

By

Al Hassan Kyakulaga
MSc, Makerere University, 2013

A Thesis
Submitted to the Faculty of the
School of Medicine of University of Louisville
in Partial Fulfillment of the Requirements
for the Degree of

Master of Science
In Pharmacology and Toxicology

Department of Pharmacology and Toxicology
School of Medicine
University of Louisville
Louisville, KY, USA

May 2017

WITHAFERIN A SYNERGISTICALLY ENHANCES THE EFFECT OF PACLITAXEL AGAINST LUNG CANCER

By

Al Hassan Kyakulaga

MSc. Makerere University, 2013

A Thesis Approved on

February 09, 2017

By the following thesis committee:

Ramesh C. Gupta, Ph.D.

Jason Chesney, M.D., Ph.D.

Jun Yan, M.D., Ph.D.

Frederick A. Luzzio., Ph.D.

Chee M. Ng, Pharm D., Ph.D.

Farrukh, Aqil, Ph.D.

ACKNOWLEDGEMENTS

I would like to extend my sincere gratitude to my mentor Dr. Ramesh Gupta for his continuous guidance and financial support towards my academic and professional career development. My acknowledgments go to Drs. Farrukh Aqil, and Radha Munagala for their tireless efforts towards teaching me all skills that have enabled me to accomplish this work. I am also thankful to my lab mates - Jeyaprakash Jeyabalan, Ashley Mudd, Divya Karukonda and Dr. Ashish Agrawal for the continuous support they have rendered to me during the conduct of these experiments. Lastly, I would like to thank the Department of Pharmacology and Toxicology, Integrated Programs in Biomedical Sciences (IPBS) program, the Agnes Brown Duggan Endowment, and the School of Graduate Studies at the University of Louisville for the Graduate Fellowship and other financial support.

ABSTRACT

WITHAFERIN A SYNERGISTICALLY ENHANCES THE EFFECT OF PACLITAXEL AGAINST LUNG CANCER

Al Hassan Kyakulaga

February 09, 2017

Lung cancer is the leading cause of cancer-related deaths among both men and women in the U.S and worldwide. Today, paclitaxel (PAC) or taxol alongside platinum-based drugs is the most widely used agent as first-line regimen for advanced NSCLC. However, due to toxicity, drug resistance, solubility and efficacy issues, efficacy has plateaued. In the present study, the potential of a novel plant-derived steroidal-lactone, withaferin A (WFA), for clinical use alongside PAC to improve efficacy against NSCLC was explored. The anticancer effects of PAC and WFA alone, and in combination against the *in vitro* cell proliferation, cell adhesion, migration and invasion of two human NSCLC cell lines, H1299 and A549 were determined. Our data shows that PAC and WFA, combined at 1:25 and 1:50 ratios, respectively, synergistically inhibited the proliferation of H1299 and A549 cells. Furthermore, the combination also significantly inhibited the TGFβ1-induced EMT, cell adhesion, migration, and invasion ($p<0.05$) indicating a potential anti-metastatic activity. Together, if these findings can be replicated in appropriate animal models, they highlight the potential clinical efficacy of WFA alongside PAC that can be exploited to improve clinical outcomes of NSCLC treatment.

TABLE OF CONTENTS

LIST OF FIGURES

INTRODUCTION

Lung cancer has an extremely low survival rate and is currently the leading cause of cancer-related deaths worldwide and in the US [1-3]. It is estimated that (see Figure 1) over 1.8 million new cases and 1.6 million deaths occur worldwide annually [2] of which an estimated 221,200 cases and 158,040 deaths occur in the U.S [3, 4]. Despite the recent advances in imaging and molecular diagnostic techniques, targeted therapies and immune checkpoint inhibitors, the overall 5-year survival rate for lung cancer has remained less than 17%. Overall more people die from lung cancer than from breast, prostate, pancreatic and colon cancers combined [3].

This extremely poor prognosis of lung cancer is explained in part because, in the early stages, lung cancer is not associated with any major clinical symptoms [5]. Consequently, the majority (60-70%) of patients are diagnosed when the disease is in its late stages [2] and is associated with regional and/or distant metastases for which surgery and radiation are almost impossible [6]. Even among patients with sufficiently localized tumors, more than half of them have additional cardiac or pulmonary diseases that complicate the therapeutic options. Furthermore, it is widely reported that 50-60% of patients who undergo initial successful surgical resection of primary tumors relapse within 6-12 months [7].

Together, the advanced stage of lung cancer among most patients, high relapse rates, tumor cell heterogeneity, biological aggressiveness and intrinsic resistance to chemotherapy make lung cancer very challenging to treat.

Clinically, lung cancer is not a single disease but refers to a heterogeneous group of tumors that originate from the lung tissue [5]. These tumors almost exclusively (>99%) develop from epithelial cells lining the airways, and as such are also called lung carcinomas [5, 8]. Their carcinogenesis is complex, but multiple lines of evidence suggest that normal airway epithelial cells are transformed into lung carcinomas via a multistep carcinogenic process involving the interaction of genetic, environmental and lifestyle factors [3, 9, 10]. It is hypothesized that exposure to carcinogens causes specific genetic and/or epigenetic alterations that confer a proliferative advantage to a small number of cells. Later, these cells get progressively transformed into biologically aggressive and highly malignant tumors that are associated with extremely poor prognosis and high mortality rates [5].

Based on cellular morphology, lung cancer is classified as either small-cell lung cancer (SCLC) or non-small-cell lung cancer (NSCLC) [11]. Current statistics indicate that only 10-13% of the cases are SCLC while the majority (80-85%) are NSCLC [5, 12]. SCLC tumors (Figure 2F) are reported to primarily occur among heavy smokers, and they are histologically identified as small round-shaped cells, with visible mitotic patterns, granular nuclear chromatin and absent nucleoli [10]. On the other hand, NSCLC tumors are more prevalent among non-smokers and are further sub-divided into three major subtypes: adenocarcinoma, squamous cell carcinoma and large cell lung cancer [5, 13, 14]. The adenocarcinomas are

currently the most prevalent subtype of NSCLC especially among non-smokers and women [2, 10]. Histologically, adenocarcinomas (Figure 2A-C) are the NSCLC tumor cells that appear microscopically as either glandular or mucin-producing cell, and are usually arranged as acinar, papillary, bronchoalveolar, solid or a mixture of these growth patterns. In contrast, squamous cell carcinomas which are the second most prevalent subtype of NSCLC tumors are identified as NSCLC tumor cells that display intercellular bridges and keratin (Figure 2D). The large-cell carcinomas (Figure 2E) present as large NSCLC tumor cells that contain vesicular nuclei and prominent nucleoli. Worldwide, these traditional classifications have been widely utilized in decision making for treatment strategies for lung cancer.

Unfortunately, in the current era of precision and personalized medicine [14], the histologic classifications of NSCLC are somewhat insufficient and may not reflect the underlying driver mutations. Therefore, today NSCLC tumors are also subtyped using immunohistochemical and molecular techniques to reflect the genetic mutations that drive and maintain tumorigenesis [15]. Many clinical reports indicate that adenocarcinomas are usually associated with mutations in the EGFR, KRAS, and ALK genes [2, 10, 16]. On the other hand, squamous-cell carcinomas have mutations in SOX2, FGFR1, TP53 and DDR2 genes while small-cell lung cancers display RB1, TP53 mutations [16]. These molecular classifications allow for effective and tailored treatments for specific subsets of patients [14, 17].

The causes of lung cancer remain elusive but several risk factors have been identified in epidemiological studies. To date, cigarette smoking remains the major cause of lung cancer and the global patterns of lung cancer incidence closely

reflect the consumption rates of tobacco products in many countries [5]. In the U.S, more than half of the newly diagnosed lung cancer cases are directly attributable to smoking and it is estimated that over 90 million people are at risk of smoking-related lung cancer [1]. Data from several epidemiological studies indicate that the risk of lung cancer increases with both quantity and duration of smoking, and is highest among those who smoke and never quit [3, 5, 10, 15]. Furthermore, evidence has also increased indicating that side-stream cigarette smoke exposure or the so-called “passive smoking” also increases the risk of lung cancer and accounts for a large fraction of lung cancer among non-smokers [2]. Interestingly, despite the widespread anti-smoking campaigns and the observed declines in smoking rates in developed countries, the incidence and mortality rates of lung cancer have only moderately decreased. The American Cancer Society (ACS) has estimated that the incidence of lung cancer decreased by only 2% among men and 1% among women per year between 2004 and 2013 [3].

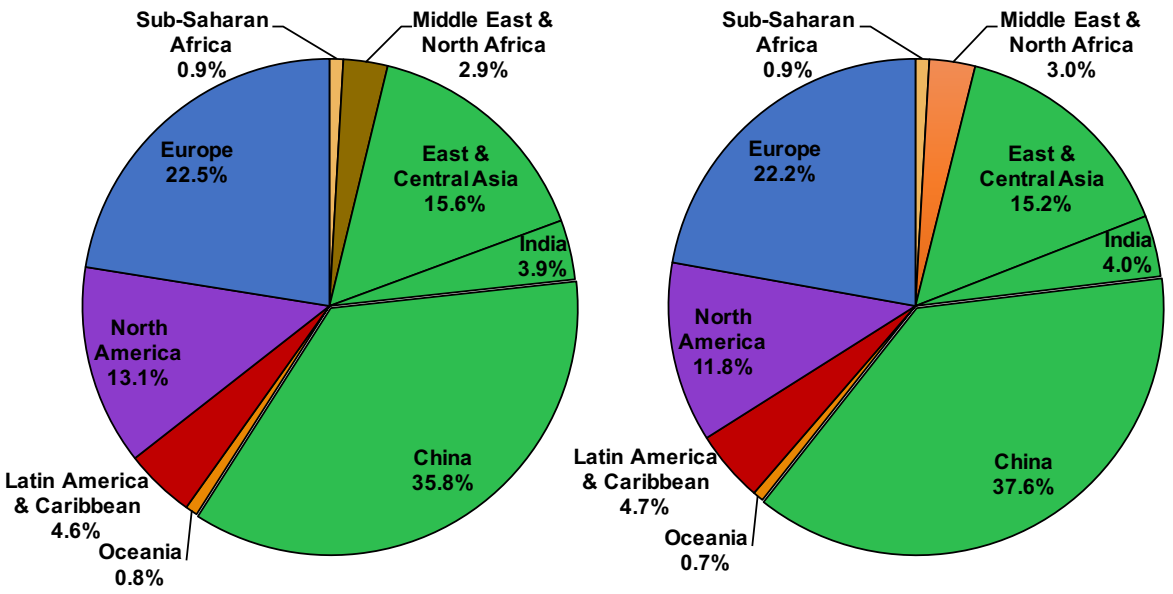

Figure 1. The worldwide estimated global number of new cases and deaths with proportions by major world regions for lung cancer. (Source: Stewart B.W. and Wild P.S: World Cancer Report, 2014).

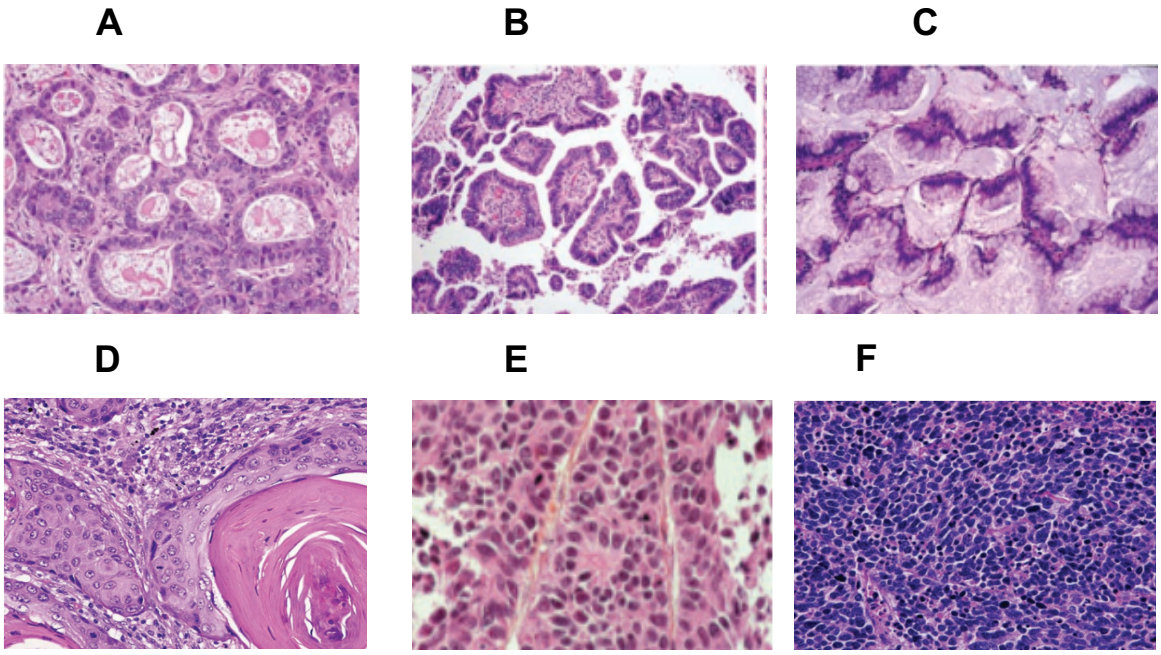

Figure 2. Histologic classifications of lung cancer: (A) acinar adenocarcinoma, (B) papillary adenocarcinoma (C) invasive mucinous adenocarcinoma (D) squamous-cell carcinoma (E) large-cell carcinoma and (F) small-cell carcinoma (Source: Stewart B.W. and Wild P.S (2014). World Cancer Report, 2014).

Today, the therapeutic options and clinical outcomes of lung cancer treatment are highly dependent on the stage of the disease at the time of diagnosis [6, 13, 18]. Initially, a proper and accurate diagnosis is done to consider the size and location of the primary tumor, as well as the presence of regional and/or distant metastases. Later, the data obtained from the initial screening is used to stage the lung cancer and to select the suitable therapeutic options for each patient [2]. The World Health Organization (WHO) utilizes and recommends the Tumor-Node-Metastasis (TNM) staging system of lung cancer based on the size of the primary tumor(T), regional lymph nodes (N), and (M) distant metastases [19, 20]. Using this system, a combination of TNM descriptors is used to group lung tumors into seven stages that reflect expected survival outcomes [11].

The seven clinical stages of lung cancer used the world over are; IA, IB, IIA, IIB, IIIA, IIIB and V. Here, the best therapeutic outcomes expected from stage I and the worst outcome from stage V [19]. Many clinical reports indicate that the stages IA, IB, IIA, IIB are considered early stage lung cancer [20, 21] where the primary tumors are sufficiently localized and therefore are considered curable. However, patients with stages III-V are considered to have advanced lung cancer and thus have the worst clinical outcome [20]. The dismal survival for patients with advanced lung cancer is mainly because of the regional and distant metastases.

Following lung cancer staging, the therapeutic strategies for NSCLC may include surgery, chemotherapy, and radiation either alone or in combination [6, 13]. The ultimate choice of any one of these treatment options is based on whether the clinical goal is cure or palliation. For patients with early stage NSCLC (stage I-

II), surgical removal of tumors is the treatment of choice, for which cure is attainable in up to 80% and 50% for stage I and stage II cases, respectively [13]. However, even with improved diagnostic techniques, only 25% of lung cancer patients are diagnosed with stage I and stage II of the disease [2]. Moreover, a majority (50-60%) of the patients that present with early-stage lung cancer also have impaired pulmonary and cardiac functions which make them ineligible for surgery because of possible postoperative complications [6].

In contrast, about 35% and 40% of lung cancer patients are diagnosed with stage III and stage IV lung cancer, respectively [2]. Among these patients, the primary tumor is already spread beyond the lung tissue into lymph nodes (stage III) and sometimes with distant metastases (stage IV). Very frequently, advanced lung cancer patients also have undetected systemic micrometastases that can result in tumor relapse [13, 18, 22]. Therefore, the main clinical goal of treatment in advanced lung cancer is palliation of symptoms and to prolong the life of patients. Because surgery is virtually impractical, either chemotherapy or targeted therapy, alone or in combination are the viable options [18, 23].

Currently, the platinum-based chemotherapies consisting of either cisplatin or carboplatin are the first-line drugs for the treatment of advanced NSCLC [6]. Usually, these platinum drugs are administered in combination with a third-generation chemotherapeutic drug like paclitaxel, docetaxel, or vinorelbine [18, 23]. Several published studies and clinical reports indicate that the various drug combinations of platinum drugs and other chemotherapeutics show similar clinical efficacy but distinct toxicities [6, 24]. However, a two-drug combination of

carboplatin and paclitaxel is the most widely used standard chemotherapeutic regimen for stage IIIB-IV lung cancer with 1-year survival rate exceeding 40% [4, 24]. Unfortunately, the survival efficacy of the platinum-paclitaxel combination seems to have reached a survival plateau of about 10 to 11 months and thus a three-drug combination is now recommended [24]. More recently, because of the lower toxicity profile of gemcitabine, a three-drug combination consisting of carboplatin, paclitaxel, and gemcitabine was introduced with promising but minimal results [24]. In other clinical reports, pemetrexed, a more specific cytotoxic agent is recommended as the third drug to the cisplatin-paclitaxel combination with survival rates between 13-14 months [6].

In the past decade or so, there has been considerable progress in understanding the biology of lung and other cancers [17]. This led to the discovery of molecular mutations that drive the progression of cancers and subsequently the introduction of targeted therapies into clinical practice [14, 25]. These targeted therapies interact with specific molecular drivers involved in carcinogenesis, cell proliferation, apoptosis, and metastasis of cancer cells. Several reports indicate that the most promising agents for lung cancer are those agents targeting receptor tyrosine kinases (RTKs), mitogen-activated protein kinases (MAPKs) and Janus kinase (JNK) pathways [4, 14, 17]. Indeed, agents targeting EGFR mutations (erlotinib and gefitinib), ALK gene rearrangements (crizotinib and ceritinib), HER2 mutations (trastuzumab) and angiogenesis (bevacizumab) are currently approved as targeted therapies for NSCLC [17, 25, 26]. Furthermore, the anti-EGFR agent erlotinib is also approved by FDA as second-line agents for relapsed lung cancer.

Unfortunately, many patients who undergo targeted therapy eventually develop resistance with continued drug administration and relapse within 4-6 months [17]. Initially, patients show a favorable response to the targeted therapies but it has been found out that the prolonged administration results into secondary mutations that cause decreased binding affinity of the drugs to targets. Therefore, even with targeted therapies, only modest (14-17 months) improvement in overall survival has been observed and drug resistance is becoming a major problem [6].

The other landmark in NSCLC treatment is the manipulation of the immune system to enable the body clear tumor cells [27, 28]. This exciting discovery has been fueled by the increasing body of knowledge on tumor microenvironment and its interplay with the immune system. Today, immunotherapy is also being explored as an alternative treatment modality for lung cancer. Unlike chemotherapy, immunotherapies indirectly target NSCLC tumor by stimulating the individual's immune system [6]. Currently, two immunotherapeutic approaches are utilized, namely, the vaccination and the immune-checkpoint approaches. The vaccination approach employs either antigens or cells to stimulate T-cells to eliminate tumors while the immune-checkpoint approach uses specific monoclonal antibodies to neutralize specific tumor molecular pathways [4, 14]. Vaccines against EGF, TGFβ, and PD-1 are at different stages of advanced clinical testing with promising findings [4]. However, even with immunotherapies, the overall 5-year survival from lung cancer has continually stagnated between 15-17% worldwide.

Therefore, despite the enormous gains from chemotherapies, targeted, and immunotherapies for many cancer types, the overall gain for lung cancer has been minimal. To address this therapeutic challenge, there has been a re-awakened interest in the search for effective therapies for lung cancer from natural sources including medicinal plants, marine organisms, and microorganisms [28]. In this quest, medicinal plants have attracted significant attention because of the chemical and biological diversity of secondary metabolites represent an inexhaustible source of anticancer compounds. So far, more than 3000 plant species have been used to treat cancer and many more are under investigation. Generally, these plant-derived compounds are cost effective, abundantly available and largely non-toxic [4]. More importantly, unlike current drugs, recent evidence from preclinical and some clinical studies indicates that most plant-derived compounds target multiple pathways in the cancer cells [29].

Some of the most promising plant-derived compounds include resveratrol, epigallocatechin 3 gallate (EGCG), curcumin, apigenin, luteolin, barbamine and withaferin A (WFA) [29-31]. The Gupta lab group at the University of Louisville, among other projects, is focused on developing WFA into a useful therapeutic agent for the management of lung cancer. Building on hypotheses based on previous findings in this and other laboratories, WFA has shown excellent efficacy and potency against various cancers – lung [32-34], cervical [35], prostate [36], breast [37-39], ovarian [40] and pancreatic *in vitro* and *in vivo*. In the present study, a simple but effective strategy of combining WFA with paclitaxel against the proliferation, migration, and invasion of two human NSCLC cells was explored.

WFA is a member of the withanolides, a large group of naturally occurring 28-carbon-containing compounds [41]. Chemically, these withanolides (Figure 3B) are composed of a steroidal framework attached to a lactone ring and as a result, are sometimes referred to as 'steroidal-lactones' [42]. The steroidal part consists of 4-cycloalkane rings, 3-cyclohexane rings, and 1-cyclopentane ring. The second part, the lactone ring, is a cyclic ester which is oxidized appropriately to form a 6-membered ring [41]. This overall chemical structure can be modified either in the steroid framework or the side chains yielding a diversity of compounds.

To date, more than 300 different naturally occurring withanolides with diverse chemical and biological activities have been isolated and characterized from the *Solanaceae* plant species [43]. Of all these, WFA [4β, 27-dihydroxy-1-oxo-5β, 6β-epoxywitha-2, 24-dienolide], was the first member to be discovered and is currently the most extensively studied and characterized [42, 44-46]. Initially, it was first isolated from the leaves of *Withania somnifera* (Figure 3A) in the 1960s, and its structure was chemically elucidated shortly thereafter [42, 45, 46]. At that time, the basic extraction of WFA from the dried *W. somnifera* material was accomplished using methanol followed by purification with C-18 and Sefadex columns [45]. Later, WFA was also extracted from other plants including *Withania aristata, Dunalia spinose* and *Vassobia breviflora* [43, 46]. Because of the multiple reports on the anticancer activity of WFA, significant efforts are now being directed towards the chemical synthesis and modification of WFA [47].

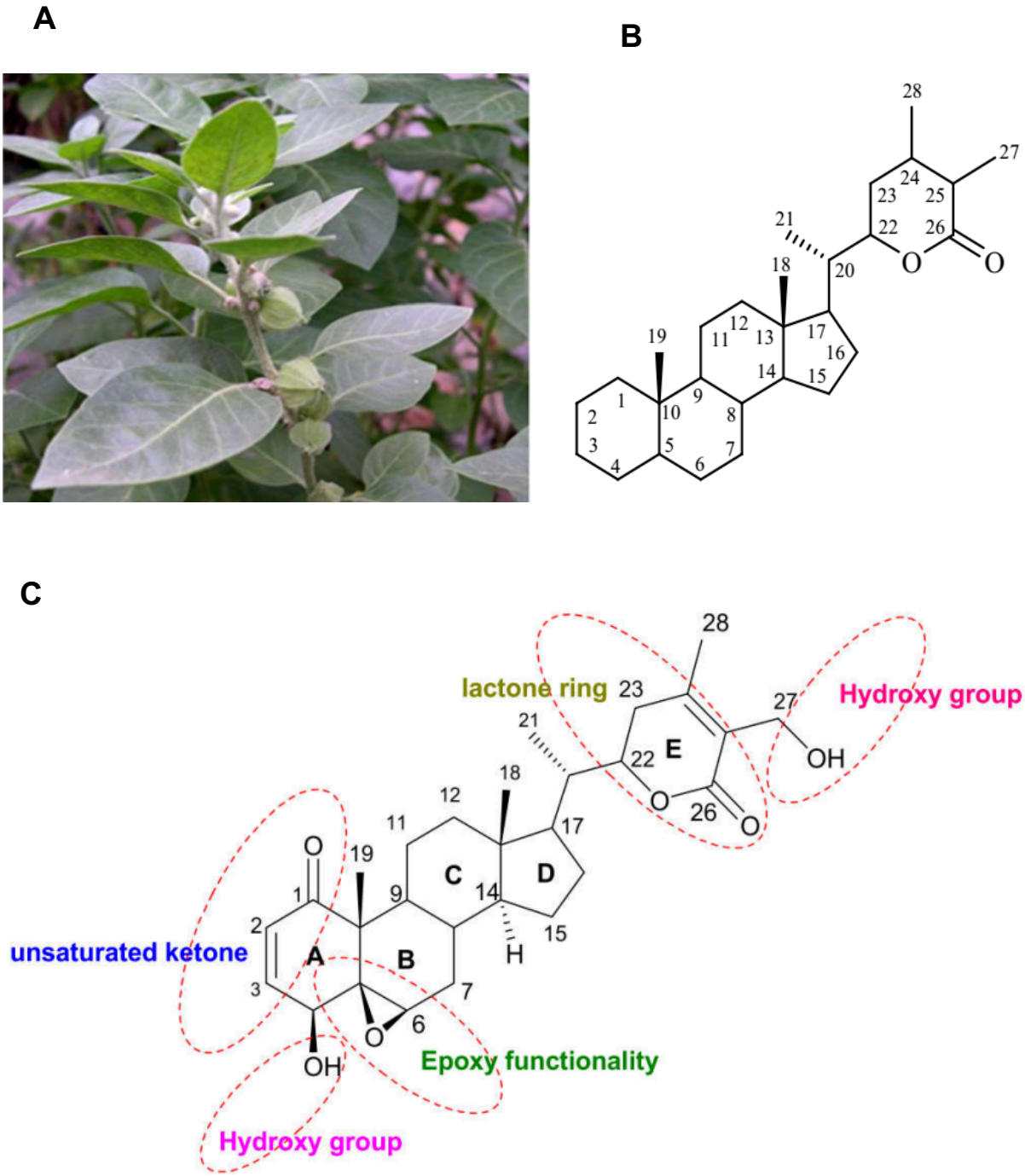

Figure 3. (A) *W. somnifera* (B) withanolide structure and (C) withaferin A [48, 49].

In the WFA chemical structure, the basic steroidal framework is ergostane, to which a lactone ring is attached (Figure 3C). As is the case for the structures of most withanolides, the lactone in WFA is a cyclic ester composed of 5-carbon atoms, which in the case of WFA, the carbon atoms at C-22 and C-26 are oxidized to form a 6-membered ring [50]. This arrangement of atoms in WFA results into five functional groups including the unsaturated ketone ring, a hydroxyl group at C-4, epoxide ring between C-5 and C-6, a hydroxyl group at C-27, a 6-carbon lactone ring, and an unsaturated carbonyl group [47, 48]. Together, these chemical functional groups account for the diverse biological activities of WFA and each may be exploited for chemical modification.

Because of its ability to interact with many molecular targets, several pharmacological activities of WFA have been identified and reported [44, 51]. These biological activities include anti-inflammatory, anticancer, antiangiogenic, cardioprotective, immunomodulatory, hepatoprotective, anticonvulsant and anabolic effects [43, 51]. However, in the past decade or so, WFA has attracted significant attention and testing mainly for its anticancer activity [44]. There is quite a plethora of data indicating the anticancer efficacy of WFA from cell culture to xenograft and orthotopic tumor models of multiple human cancers [44, 48, 51, 52].

In most of the published preclinical studies, it is reported that the observed anticancer activities of WFA result from its interaction with specific biochemical and molecular targets like enzymes, signaling molecules and other proteins in cancer cells [41, 51]. Three positions on the WFA structure have been identified to react with sulfhydryl groups of cysteine residues in proteins in cancer cells [47]. These

positions include the unsaturated ketone (C-3) in the A-ring, the epoxide group at C-5 and the lactone ring [47]. Recent spectral analysis has revealed that C-3 is the main target for thiol group binding in the unsaturated A-ring [39]. It is hypothesized that the sulfhydryl groups of cysteine residues react with C-3 via Michael-Addition alkylation type of reactions forming covalent bonds with proteins [48, 49]. Furthermore, the epoxide ring between C-5 and C-6 has been reported as the most critical for its anticancer properties of WFA. To support this hypothesis, an in vitro study investigating the reaction of WFA and 2-mercaptaethanol, which specifically affects the 5β,6β-epoxide structure, have reported a loss of anticancer activity. In the same study, incubation of WFA with strong reducing agents like N-acetyl cysteine or DTT resulted into loss of the pro-apoptotic activity of WFA [53]. On the other hand, loss of unsaturation in the A-ring have been reported to cause loss of anti-inflammatory and antiangiogenic effects of WFA [43, 54].

The mechanistic data on the anticancer activity of WFA are backed by the growing body of evidence demonstrating the preclinical efficacy of WFA against various cancer types *in vitro* and *in vivo*. Perhaps the most extensively investigated type of cancer for which WFA has shown excellent activity is breast cancer. Here, multiple lines of evidence from independent studies indicate that WFA induces apoptosis in estrogen-sensitive (MCF-7) and estrogen-independent (MDA-MB-231) breast cancer cells *in vitro* [55]. In the same study, the *in vitro* findings were corroborated by *in vivo* studies in which intraperitoneal administration of WFA (4 mg/kg) in nude mice significantly attenuated the growth of subcutaneous MDA-MB-231 xenografts. Similarly, in another study using orthotopically implanted 4T

mouse mammary tumor cells, it was reported that intraperitoneal administration of WFA (0.1, 0.5, 1, 2 and 4 mg/kg body weight) significantly inhibited breast cancer progression and metastasis in a dose-dependent manner [39, 56]. Furthermore, a study using a clinically-relevant transgenic animal model for breast cancer in MMTV-neu mice reported more than 50% inhibition of weight of palpable tumors following treatment with 100 μg of WFA (3 times/week) for 28 weeks [37, 56].

In addition to breast cancer, the evidence is available to support the efficacy of WFA against prostate, ovarian, and cervical cancers. For example, in a study conducted in nude mice, intraperitoneal administration of WFA [4-8 mg/kg/day] for 24 days resulted in over 70% inhibition of PC3 subcutaneous tumor growth [57]. The authors attributed the effects of WFA to inhibition tumor proteasomal activity and induction of apoptosis in PC3 cells. Similarly, another independent study in WFA [3 or 5 mg/kg] was administered orally to transgenic mice for 39 weeks, there was significant inhibition of tumorigenesis and metastasis of prostate adenocarcinoma [36]. In cervical cancer, data from *in vitro* and *in vivo* experiments indicates the inhibition of human papillomavirus oncogenes E6/E7 coupled with induction of p53, the tumor suppressor protein [34]. Furthermore, administration of WFA alone or in combination with cisplatin to nude mice bearing A2780 human ovarian cancer cell xenografts resulted into 70-80% reduction in tumor growth and complete inhibition of metastasis [40, 58, 59]. Together, these data demonstrate the efficacy of WFA against gynecological cancers and further highlight the potential of WFA as a potential chemotherapeutic agent.

MATERIALS AND METHODS

Materials

Culture media (1X DMEM and RPMI 1640), 0.25% Trypsin-EDTA, Bolt MES-running buffers, antibiotics (100 U/mL penicillin/ 100μg/mL streptomycin), and fetal bovine serum (FBS) were purchased from Life Technologies (Grand Island, NY). RIPA cell lysis buffer, halt protease/phosphatase inhibitor cocktail, BCA protein assay kits, PVDF-transfer membranes, ECL chemiluminescence reagents and the 10-well Bolt 4-12% Bis-Tris phosphate gels were purchased from ThermoFisher Scientific (Rockford, IL). The tissue culture treated plates (96-well, 24-well, 12-well, and 6-well) and culture treated dishes (60 mm and 100 mm) were purchased from CytoOne (USA Scientific, FL).

The 2-well culture inserts and the 8-well glass μ-slides were purchased from ibidi® cells in focus (Madison, WI). The transwell tissue culture inserts and the matrigel base membrane matrix were purchased from Corning (Bedford, MA). Recombinant human transforming growth factor (hTGFβ-1), primary antibodies (anti-E-Cadherin, anti-Vimentin, anti-Snail, anti-ZEB1, anti-β-Catenin, anti-β-actin, anti-slug, anti-Bcl2, anti-Bax, anti-PARP, anti-cyclin E_2, anti-cyclin B_1 and anti-STAT3) as well as secondary (anti-mouse IgG and anti-rabbit IgG) antibodies were purchased from Cell Signaling Technology, Inc. (Danvers, MA).

The FITC-AnnexinV/PI apoptosis assay kits were purchased from Invitrogen (Eugene, OR), while the phosphate-buffered-saline (PBS) and MTT reagent [3-(4, 5-dimethylthiazolyl-2)-2, 5-diphenyltetrazolium bromide] were purchased from Sigma-Aldrich (St. Louis, MO).

Cell lines and culture

Two human NSCLC cell lines, H1299 (p53-null, EGFR-WT) and A549 (p53-WT, EGFR-WT), originally purchased from American Type Culture Collection (Manasa, VA, USA) and sub-cultured in the laboratory were used. These cells were maintained in monolayers at 70-80% confluence in DMEM supplemented with 10% heat-inactivated FBS and 1% antibiotics at 37°C in a 5% CO_2 humidified incubator. Culture media was replaced with fresh media every 2 days and cells were passaged at >80 % confluence.

MTT cell viability assay

Cell viability was indirectly measured by MTT assay as described previously [60] using the yellow MTT reagent. In this assay, the ability of cells to metabolize the yellow tetrazolium MTT reagent to purple intracellular formazan crystals in the mitochondria was used as an indirect measure of cell viability. Briefly, H1299 and A549 cells (3000 cells/well) in 100μL of DMEM media were seeded in 96-wells plates and incubated for 24 hours at 37°C in a 5% CO_2 incubator. The seeding culture media was discarded by aspirating into a waste bottle and replaced with media containing various concentrations of either paclitaxel or WFA or the combination (1:25 and 1:50) and then incubated further for 72 hours. At the end of the desired incubation period, culture media was replaced with media containing

0.5 mg/mL MTT solution, incubated for an additional 3 hours at 37°C after which the media was discarded. To solubilize the formazan crystals, 200 µL of dimethyl sulfoxide (DMSO) was added and the absorbance of the resulting solution was determined spectrophotometrically at 570 nm.

Apoptosis analysis by flow cytometry

Apoptosis induction was analyzed by detecting phosphatidylserine (PS) translocation from the inner to the outer leaflet of the plasma membrane [61]. The calcium-dependent PS-binding protein, Annexin V (35-36 kDa), was used as a probe to determine the percentage of apoptotic cells after incubation with PAC or WFA alone and in combination. The FITC-Annexin V/PI cell staining kit (Cat. No. V13242, Invitrogen) containing a recombinant Annexin V conjugated to fluorescein (FITC), and propidium iodide (PI), a red fluorescent nucleic acid binding dye was used. In this assay, apoptotic cells present with PS flipped from the inner to the outer membrane and as such are bound by the Annexin V protein. Secondly, PI is impermeable to live cells but stains dead cells with red fluorescence by binding tightly to nucleic acids.

In the present study, H1299 and A549 cells were seeded in 60 mm culture plates and cultured to 70% confluence. Prior to incubation with drugs, cells were serum-starved for 24 hours then cultured in media containing either WFA (0.5 µM) or PAC (10 nM) or the combination at the respective concentrations for 48 hours. Following this incubation period, the cells were collected by aspirating the media and adding 1 mL of 0.25% trypsin-EDTA to each culture plate to detach the cells. The collected cells were washed twice with ice-cold PBS and suspended in 1x

Annexin-binding buffer at a cell density of approximately 1 x 10^6 cells/mL in a total volume of 100 µL. To each 100 µL of cell suspension, 5 µL of FITC-Annexin V and 1 µL of 100 µg/mL PI solution were added and incubated for 15 minutes at room temperature in the dark. Each AnnexinV/PI stained cell suspension was then diluted with 400 µL of 1x Annexin binding buffer and immediately analyzed for fluorescence using a flow cytometer by measuring the fluorescence emission at 530 nm and >575 nm. Early apoptotic cells showed green fluorescence, dead cells had red and green fluorescence while live cells showed little fluorescence. A total of 10,000 cells were counted in each cell suspension and the data expressed as percentage early and late apoptotic cells.

Cell adhesion assay

The cell adhesion assay was conducted as previously described [62] to determine the effects of PAC or WFA alone and in combination with the ability of cells to bind extracellular matrix. Briefly, 96-well plates were pre-coated with 40 µL of ice-cold 50 µg/mL matrigel solution and stored at 37 °C in a humidified incubator until used in the experiment. Also, H1299 and A549 cells were cultured in 100-mm culture dishes and allowed to grow up to 70-80% confluence. The cells were then serum starved for 24 hours, washed twice with serum-free DMEM media to remove dead cells and detached from the plates by adding 1 mL of 0.25% trypsin-EDTA. The collected cells were centrifuged at 350 x g for 5 minutes to remove debris and counted under the microscope. Cell adhesion assay was conducted by seeding 1 x 10^4 cells/well in 100 µL of serum free DMEM media (with or without TGFβ1) into the 96-well matrigel pre-coated plates. To determine the effect of PAC and WFA,

alone and in combination, at the indicated concentrations on cell adhesion, each agent was added to the cell suspension before seeding. Following cell seeding, culture plates were incubated at 37°C and 5% CO_2 for 2 hours to allow attachment of cells to matrigel. Thereafter, non-adherent cells were removed by washing twice with PBS, then 100 μL of DMEM (10% FBS) was added to each well and the plates were incubated for an additional 8 to allow recovery of cells. The cell viability of adherent cells was determined by MTT assay.

Wound healing assay

The effects of PAC and WFA, alone and in combination on motility of H1299 and A549 cells were determined by wound healing assay. This experiment was performed using the 2-well tissue culture inserts (ibidi® cells in focus) following manufacturer's instructions. Briefly, H1299 and A549 cells in DMEM media (10% FBS) were cultured to 70-80% confluence in 100-mm culture dishes at 37°C and 5% CO_2. At 80% confluence, cells were serum starved for 24 hours and collected by adding 1 mL of 0.25% trypsin-EDTA and centrifuged at 350 x g for 5 minutes to remove dead cells and debris. Cells were re-suspended in DMEM media, counted under a light microscope and the cell number was adjusted to 3 x 10^5 cells/mL.

To each of the 2-well culture inserts, a total of 70 µL the cell suspension (3 x 10^5 cells/mL) was added and incubated at 37°C and 5% CO_2 for 24-hours to obtain a confluent monolayer of cells in each of the chambers. Thereafter, culture inserts were removed to expose the wound area (gap) between the two cell growth areas using a pair of forceps. Floating and dead cells were removed by washing the cells twice using serum-free DMEM media, then cells cultured in serum-free

DMEM media containing PAC or WFA alone or the combination. The gap area was monitored by examining the cells under a light microscope immediately (0-hours) and after 24 hours post treatment. The percent migration in each microphotograph was determined using Wimasis Image Analysis software (WimScratch).

Transwell cell migration and invasion assay

The effects of WFA and PAC, alone and in combination on transwell migration and invasion of human NSCLC cells were determined using 8-μm pore size transwell culture inserts. Briefly, H1299 or A549 cells (8×10^5 cells/plate) were cultured in 100-mm culture plates in DMEM media (10% FBS) to 70-80% confluence. Thereafter, cells were serum starved for 24 hours and detached from plates using 0.25% trypsin-EDTA, suspended in serum free media and counted.

To conduct the transwell migration assay, 2.5×10^4 cells in 200 μL of serum free DMEM media (with and without TGFβ1 in presence or absence of PAC or WFA alone and in combination) were seeded in the upper chamber of the transwell insert. A total of 600 μL of DMEM (10% FBS) was added to the bottom chamber to act as an attractant to cause cell migration. After 24-hour incubation, the migrated cells at the bottom of the insert were washed twice with PBS and fixed using 3.7% paraformaldehyde at room temperature for 10 minutes. The fixed cells were washed twice using PBS, permeabilized using 100% methanol for 20 minutes at room temperature and stained using 0.2% toluidine blue (in 1% sodium borate) for 15 minutes. The non-migrated cells remaining in the upper chamber of the transwell insert were removed using a cotton swab, and the number of migrated cells counted under the microscope. In the matrigel invasion assay, the same

procedure was followed except that the upper chamber of each transwell insert was pre-coated with 40 µL of 3.0 mg/mL matrigel at 4°C prior to cell culture. The number of migrated cells for each experimental unit was compared with the number of migrated cells in the control group.

Western blot analysis

Western blotting was performed to compare expression levels of specific proteins in H1299 and A549 cells following incubation with either WFA or PAC, alone and in combination. In each experiment, cells were cultured up to 70-80% confluency and then incubated with either WFA or PAC, alone and in combination as indicated. The cells were collected using 0.25% trypsin-EDTA and washed twice with PBS at 4°C. Whole-cell protein lysates were prepared by suspending collected cell pellets into 50-100 µL of RIPA buffer and incubated for 30 minutes on ice. Thereafter, cells were lysed by vortexing the cell suspension for 30 seconds and protein lysate collected by centrifugation at 17000 x g for 45 minutes. The supernatant for each sample was transferred into labeled pre-chilled 1 mL tubes and the total protein concentration for each sample was determined by BCA method. For detection of specific proteins, volumes containing 20 µg of protein were loaded and separated per molecular weight on sodium dodecyl sulfate-polyacrylamide gel electrophoresis (SDS-PAGE) using Bolt electrophoretic apparatus following manufacturer's instructions.

Pre-stained proteins (10 µL) were loaded alongside the samples and used as molecular weight markers on either side of the gel during electrophoresis. The separated proteins were transferred from the gels onto PVDF membranes using a

Bio-Rad Transblot Cell apparatus at 20mV for 20 minutes. The membranes were washed in Tris-buffered-saline containing 0.1% Tween-20 (TBST) buffer for 5 minutes and blocked with 5% non-fat milk prepared using TBST for 1 hour. After 3 wash cycles (5 minutes each) in TBST, blots were cut according to protein molecular weight and the respective blots were incubated with primary antibodies in 10 mL of 5% non-fat dry milk (1:1000) at 4° C overnight. The following day, blots were washed 5 times in TBST (10 minutes each) to remove unbound primary antibodies and then incubated with respective HRP-conjugated secondary antibodies in 5% non-fat dry milk (1:3000) for 1 hour at room temperature. The primary and secondary antibody solutions were collected into 15 mL tubes and stored at -80°C for use in other experiments. The expression levels of each protein were determined by visualizing protein bands on blots using ECL detection reagents (Thermo Scientific) and images for each blot were developed. β-actin (for total protein) was used as protein loading control in all the experiments.

Data and statistical analysis

In all experiments, vehicle and positive control groups were used to assess the validity of experimental conditions. Data were presented as means ± SD of technical replicates from at least 3 separate experiments. Normality and homogeneity of variances for all data sets were determined before conducting to one-way ANOVA. Comparisons of experimental versus vehicle control groups were done using the student's t-test and p-values <0.05 were considered statistically significant.

Calculation of synergism between PAC and WFA

The synergistic interaction between PAC and WFA was determined using the combination index (CI) method developed Chou et al., [63]. In this method, the fraction affected (f_u) and the fraction unaffected were used to represent the percentage of cells killed by drug and the percentage of viable cells, respectively at each dose (D). For either PAC or WFA, the relationship between D, f_a, f_u and D_m was expressed in the median-effect equation (1) below;

$$\frac{f_a}{f_u} = \left(\frac{D}{D_m}\right)^m \qquad \text{Equation (1)}$$

where; m is the shape of the dose-effect curve, and D_m is the median inhibitory concentration (IC_{50}). Using equation (1), the dose (D_x) of either PAC (i.e. D_{xPAC}) or WFA (i.e. D_{xWFA}) alone that caused a specific inhibitory effect x% on the individual dose-response curves could be estimated by rearranging Equation (1) as follows;

$$D_x = D_m \left(\frac{f_a}{f_u}\right)^{1/m} \qquad \text{Equation (2)}$$

Further, the doses of PAC (D_{PAC}) or WFA (D_{WFA}) in the combination contributing to the same inhibitory effect (x%) as the individual agents was estimated from the combination dose-response curves using Equation (2). Equation (1) was further expressed in the logarithmic form as Equation (3) to enable the calculation of either D_m or D whenever other values of the equation were known.

$$\log\left(\frac{f_a}{f_u}\right) = \log\left(\frac{D}{D_m}\right)^m = m\log \text{ —— } m\log(D_m) \quad \text{Equation (3)}$$

Synergism at a specific effect levels (e.g. 50%, 75% or 90%) was determined by calculating the combination index (CI) using Equation (4), that essentially compared the doses; D_x (drug alone) and D (drug in the combination) for both PAC and WFA required to produce the same effect.

$$CI = \left(\frac{D_{PAC}}{D_{xPAC}}\right) + \left(\frac{D_{WFA}}{D_{xWFA}}\right) \quad \text{Equation (4)}$$

where; D_{PAC} and D_{WFA} were the doses of PAC and WFA, respectively in the combination while, D_{xPAC} and D_{xWFA} were the doses of PAC and WFA alone, respectively at the selected effect level. The CI values; CI<1, C=1 and C>1 indicated synergism, additive and antagonism, respectively. All these calculations were performed using CalcuSyn Version 2.0 software.

RESULTS

Antiproliferative activity of PAC and WFA against H1299 and A549 cells

NSCLC cells are reported to be highly proliferative tumor cells that are usually resistant to standard chemotherapeutic agents. Therefore, targeting cell proliferation is a therapeutically viable strategy for developing clinically effective drugs. The objective of the present study was to determine and compare the effects of PAC and WFA alone, and in combination on the proliferation of two human adenocarcinoma cell lines, H1299 and A549. Cells were incubated with PAC or WFA alone and in combination for indicated time points and cell viability was determined by MTT assay. The hypothesis was that PAC as the standard-of-care therapeutic, when used in combination with WFA would result into significantly enhanced antiproliferative activity and/or decrease the concentration of PAC required to achieve similar or higher anticancer effects. The dose-response data was used to calculate the median inhibitory concentrations (IC_{50}) of either PAC or WFA alone and in combination.

Figure 4A depicts the dose-response curves for PAC [0-40 nM] and WFA [0-2000 nM] alone against the proliferation H1299 and A549 NSCLC cells. It was observed that PAC alone had a dose-dependent inhibitory effect on proliferation of both H1299 and A549 cells. For the two cell lines, concentrations of PAC alone (less than 5 nM) displayed similar antiproliferative activities as indicated by the shape of

the dose-response curve. However, at PAC concentrations of 8 nM and greater, there was more antiproliferative activity against A549 cells than towards H1299 cells. The IC_{50} values of PAC were 8 nM and 25 nM against A549 cells and H1299 cells, respectively. Despite the remarkable potency of PAC against either cell lines, the maximum achievable inhibitory effect (or efficacy) for PAC was less than 80% for the doses tested in this experiment.

Similarly, WFA also displayed dose-dependent inhibitory antiproliferative effects against both H1299 and A549 cells. Based on data from the dose-effect plot approximations, at WFA concentrations less than 800 nM, both H1299, and A549 cells had similar percent viability. However, as WFA concentrations increased to 1000 nM and greater, there was a greater antiproliferative activity of WFA towards H1299 cells than A549 cells. The overall IC_{50} values of WFA were 831 nM and 683 nM against A549 and H1299 cells, respectively. Unlike PAC, at the tested concentrations, the efficacy of WFA was greater than 90% against both cell lines. Together, these results indicated that PAC had higher potency but lower efficacy than WFA against both cell lines at the tested concentrations.

Based on the results of the antiproliferative activity of PAC and WFA alone, it was hypothesized that the combination of PAC and WFA would have greater antiproliferative effects than each agent alone. Initially, both cell lines were incubated either PAC (10 nM) or WFA (0.5 μM) alone and in combination and the cell viability was determined at multiple time points. Figure 4B shows the time-dependent antiproliferative activity of PAC and WFA at multiple time points.

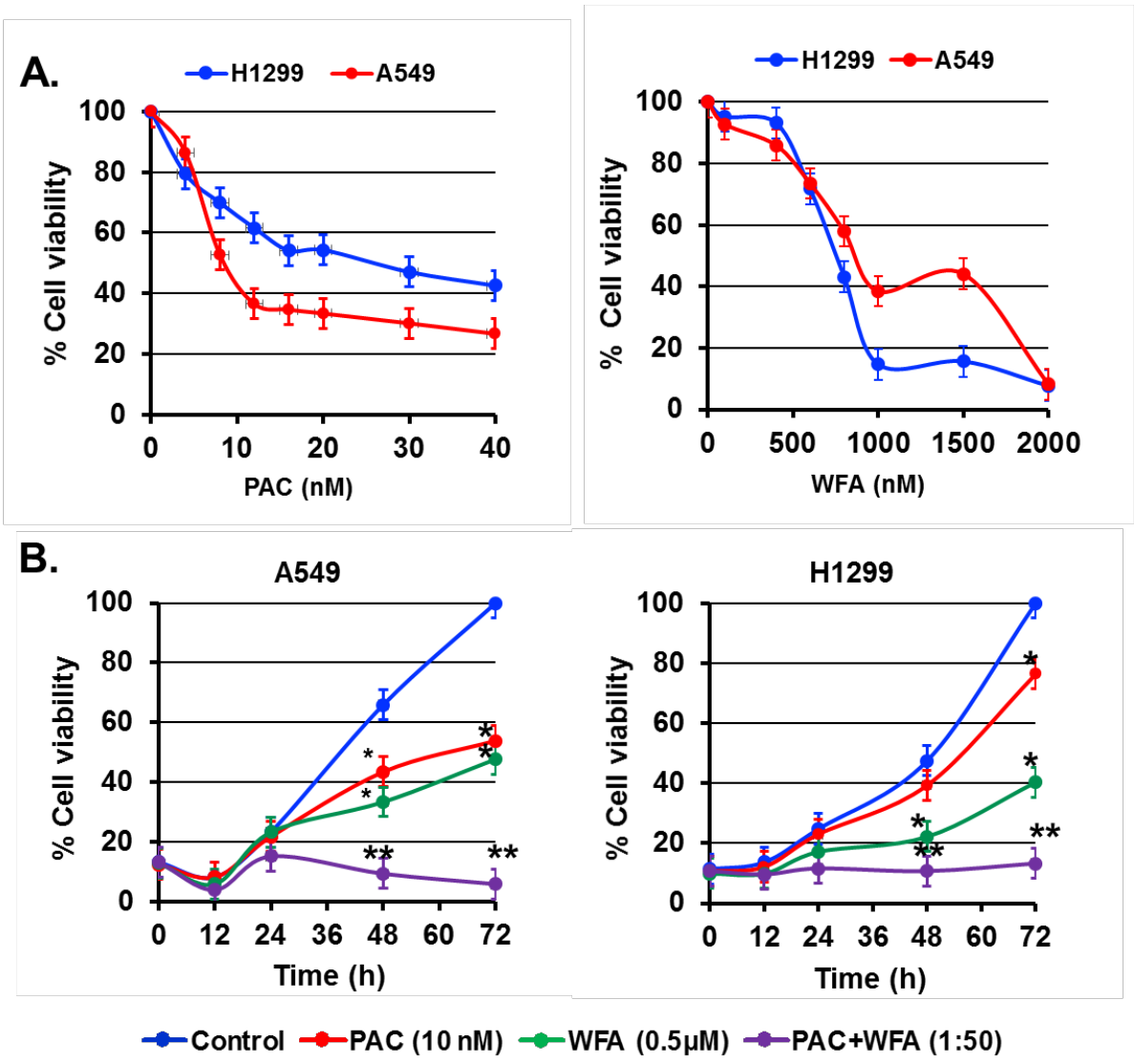

Figure 4. Antiproliferative activity of PAC and WFA, alone and in combination against H1299 and A549 NSCLC cells *in vitro*. (**A**) The dose-response effects of PAC and WFA alone against H1299 and A549 cells respectively. The cells were cultured in DMEM media in 96-wells culture plates and incubated with PAC [0-40 nM] or WFA [0-2000 nM] for 72 hours. The IC_{50} of PAC were 8.1 and 25 nM while the IC_{50} for WFA were 831 and 683 nM against A549 and H1299 cells, respectively. (**B**) The time-dependent antiproliferative activity of PAC [10 nM] or WFA [0.5 μM] alone and in combination against A549 and H1299 cells. Both PAC and WFA alone decreased the viability of cells especially at 48 and 72 hours (*$p<0.05$). The combination of PAC and WFA had a greater inhibitory effect than either PAC or WFA alone (**$p<0.001$). Data are mean ± SD values (n=8).

WFA synergizes the anticancer effects of PAC against H1299 and A549 cells

To investigate whether the antiproliferative activities of the combination of PAC and WFA was synergistic, the dose-response data of PAC or WFA alone and in combination was subjected to synergism analysis using the method described by Chou et al., [63]. Figure 5A shows the dose-response plots of PAC and WFA alone and in combination (1:50) against H1299 cells. The results indicate that both PAC and WFA alone had dose-dependent inhibitory effects on the proliferation of H1299 cells. Interestingly, for concentrations less than 12 nM, PAC alone displayed higher inhibitory effects on cell proliferation than WFA. However, the overall maximum inhibitory effect on cell proliferation was only about 60-70% for PAC while that of WFA was >90% for concentrations equal or greater than 2 μM. Together, these results demonstrate that PAC shows higher potency but lower efficacy than WFA against the proliferation of H1299 cells.

When PAC was combined with WFA, the inhibitory effects on H1299 cell proliferation was dramatically increased and there was a change in the shape of the dose-response curve. Figure 5B depicts the CI versus fractional effect plot of the combination of PAC and WFA at a combinatorial ratio of 1:50, respectively. For fractional effects between 0.2 and 1.0, the CI values were all below 1 indicating a synergistic interaction between PAC and WFA. Figure 5C shows the summary of CI values at IC_{50}, $IC_{75,}$ and IC_{90} which were 0.8, 0. 8, and 0.8, respectively for the combinatorial ratio of 1:50. Similarly, at the combinatorial ratio of 1:25, the CI values at IC_{50}, IC_{75} and IC_{90} were 0.8, 0.6, and 0.6 respectively. The overall IC_{50} values for PAC and WFA combination were 7 and 10 nM at 1:50 and 1:25 ratios.

Similarly, against A549 cells, as shown in figure 6A, PAC and WFA alone had dose-dependent inhibitory effects on cell proliferation with maximum effects of 70% and >80% for PAC and WFA, respectively. The combination of PAC and WFA had greater dose-dependent inhibitory effects on cell proliferation than each agent used alone. Moreover, greater than 80% of A549 cell proliferation was achieved with concentrations of PAC and WFA less than 20 nM and 1 μM, respectively.

Figure 6B shows the CI versus fractional effect plot of the combination of PAC and WFA at a combinatorial ratio of 1:50. As indicated, there was a dramatic decrease in the concentration each agent required to achieve specific inhibitory effects against A549 cells. The combination of PAC and WFA had CI values less than 1 for fractional effects between 0.2 and 1.0 against both H1299 and A549 cells. This indicated that the interaction of PAC and WFA was synergistic at 1:50 combination ratio. In summary, table 1 indicates that for H1299 cells, the combination achieved a 3-fold and 4-fold reduction in the IC_{50} values of PAC when it was combined with WFA. Moreover, at higher inhibitory effects (75% and 90%), there was an even greater dose reduction for PAC of up to 8-fold and 17-fold, respectively. Similarly, in A549 cells, specific inhibitory effects (50%, 75%, and 90%) were achieved with much lower paclitaxel concentrations (3-fold, 12-fold, and 46-fold), respectively.

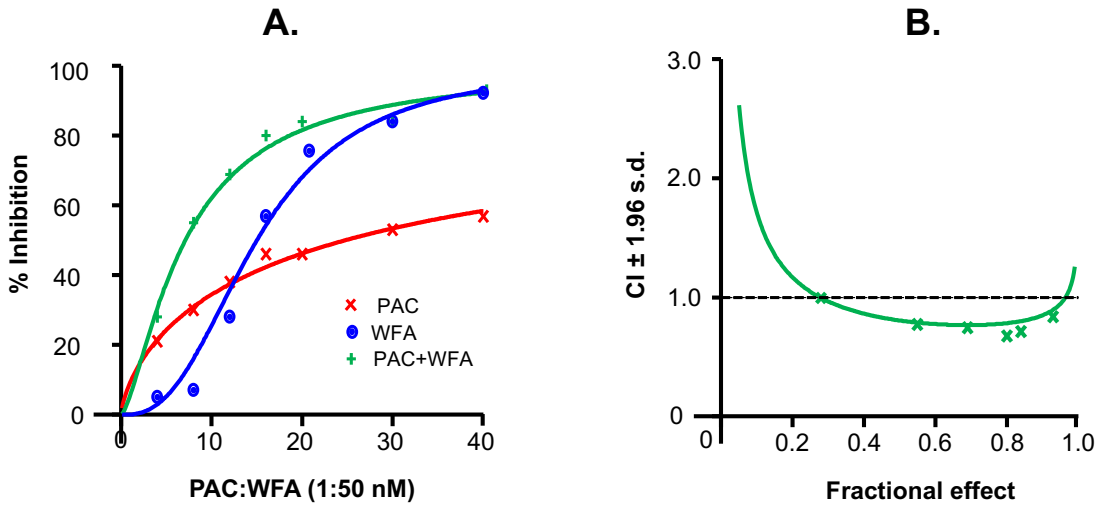

C.

Test agent	Combination Index			$IC_{50\ (nM)}$	m	r
	ED50	ED75	ED90			
PAC	N/A	N/A	N/A	24.7	0.7	0.99
WFA	N/A	N/A	N/A	683	2.0	0.91
PAC+WFA (1:50)	0.81	0.77	0.85	7.1	1.4	0.98
PAC+WFA (1:25)	0.78	0.62	0.59	10.2	1.5	0.98

Figure 5. The synergistic antiproliferative activity of PAC and WFA against H1299 NSCLC cells. (**A**) The percent inhibition versus concentration of PAC or WFA alone and in combination. There were dose-dependent inhibitory effects for both PAC and WFA on cell proliferation. PAC had a higher potency than WFA at concentrations lower than 12 nM but the maximum inhibition was <60% and about 90% for PAC and WFA, respectively. The combination of PAC and WFA (1:50) had much greater potency and efficacy than either PAC or WFA alone. (**B**) The CI versus fractional effect plot shows that CI < 1 for fractional effects 0.2 to 1.0 indicating synergism of PAC and WFA as calculated by CalcuSyn Software (CI<1). (**C**) The summary of CI values (<1) at IC_{50}, IC_{75}, and IC_{90} indicating synergism between PAC and WFA.

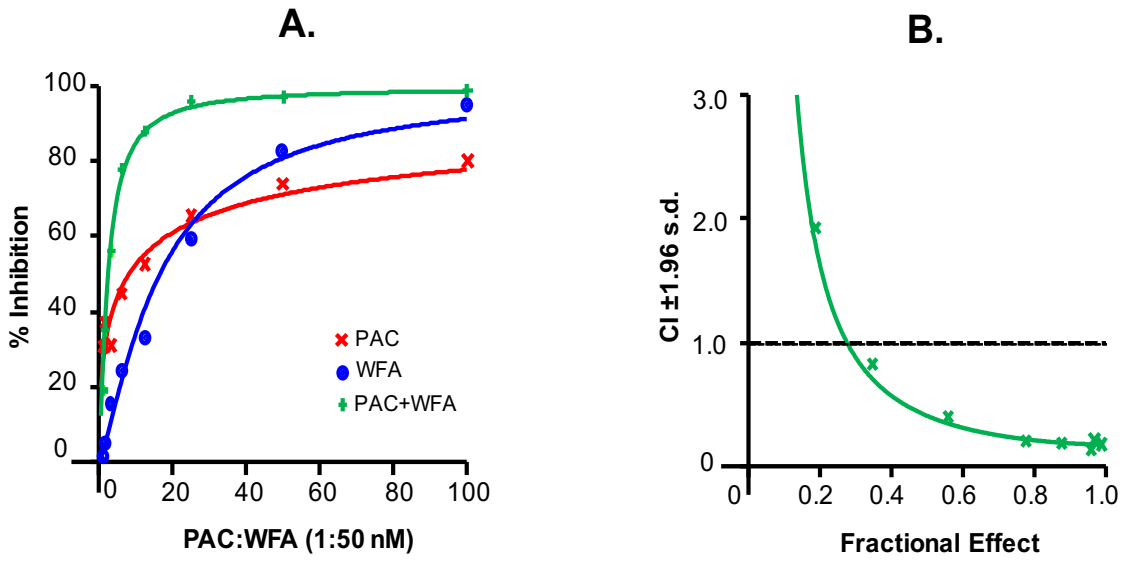

C.

Test agent	Combination Index			$IC_{50\ (nM)}$	m	r
	ED50	ED75	ED90			
PAC	N/A	N/A	N/A	8.1	0.5	0.92
WFA	N/A	N/A	N/A	831	1.3	0.96
PAC+WFA (1:50)	0.45	0.24	0.18	2.5	1.24	0.99
PAC+WFA (1:25)	0.71	0.29	0.18	4.6	1.28	0.99

Figure 6. The synergistic antiproliferative activity of PAC and WFA against A549 NSCLC cells. (**A**) The percent inhibition versus concentration plot for PAC or WFA alone and in combination. There were dose-dependent inhibitory effects for both PAC and WFA on cell proliferation. PAC had a higher potency than WFA at concentrations lower than 25 nM and a maximum percent inhibition of 70% and about 90% for PAC and WFA, respectively. The combination of PAC and WFA (1:50) had much greater potency and efficacy than either PAC or WFA alone with maximum percent inhibition >95% at <10 nM PAC. (**B**) The CI versus fractional effect plot indicates CI < 1 for fractional effects 0.3 to 1.0 indicating synergism of PAC and WFA as calculated by CalcuSyn Software (CI<1). (**C**) Shows the summary of CI values (<1) at IC_{50}, $IC_{75,}$ and IC_{90} indicating synergism between PAC and WFA.

Table 1. Dose reduction of PAC in combination with WFA against NSCLC cells

		Dose of PAC (nM)		
Cell line	Effect (%)	PAC:WFA (1:0)	PAC: WFA (1:50)	PAC:WFA (1:25)
H1299	25	5	3	4
	50	25	7	10
	75	116	15	19
	90	544	32	42
A549	25	0.9	0.9	0.9
	50	8	2	4
	75	74	6	11
	90	669	15	26

Effect of PAC and WFA on induction of apoptosis in H1299 and A549 cells

Most anticancer agents including PAC halt the progression of cancer cells through the induction of apoptosis. To date, several studies have also provided evidence to show that WFA can induce apoptosis in various cancer cell types including NSCLC. To investigate whether WFA enhanced the antiproliferative activity of PAC through increased induction of apoptosis in NSCLC cells, we compared the percentage of apoptotic cells between PAC and WFA alone and in combination (1:50). Figure 7A and 7B show the Annexin V/PI dead cell assay results for cells incubated with either PAC or WFA alone and in combination. PAC alone increased the percentage of both H1299 and A549 cells positive for Annexin V stain, an indicator of increased apoptosis, with greater efficacy in A549 cells. On the other hand, WFA resulted into an increased number of Annexin V positive cells in H1299 cells more than in A549 cells. The combination of WFA and PAC resulted in a higher percentage of Annexin V positive cells for both H1299 and A549 cells than either PAC or WFA alone. The induction of apoptosis was also determined by western blot analysis of whole-cell lysates for increased levels of cleavage of PARP, a product of active caspases (Figure 7C).

In figure 8, western blot analysis revealed that WFA increased the levels of the pro-apoptotic protein Bax while decreasing the levels of the anti-apoptotic protein Bcl-2. Similarly, cell cycle regulatory proteins (cyclin E and cyclin B) were significantly decreased, indicating possible cell cycle arrest and induction of apoptosis. Overall, the combination of PAC and WFA induced apoptosis probably through cell cycle arrest by inhibiting the expression.

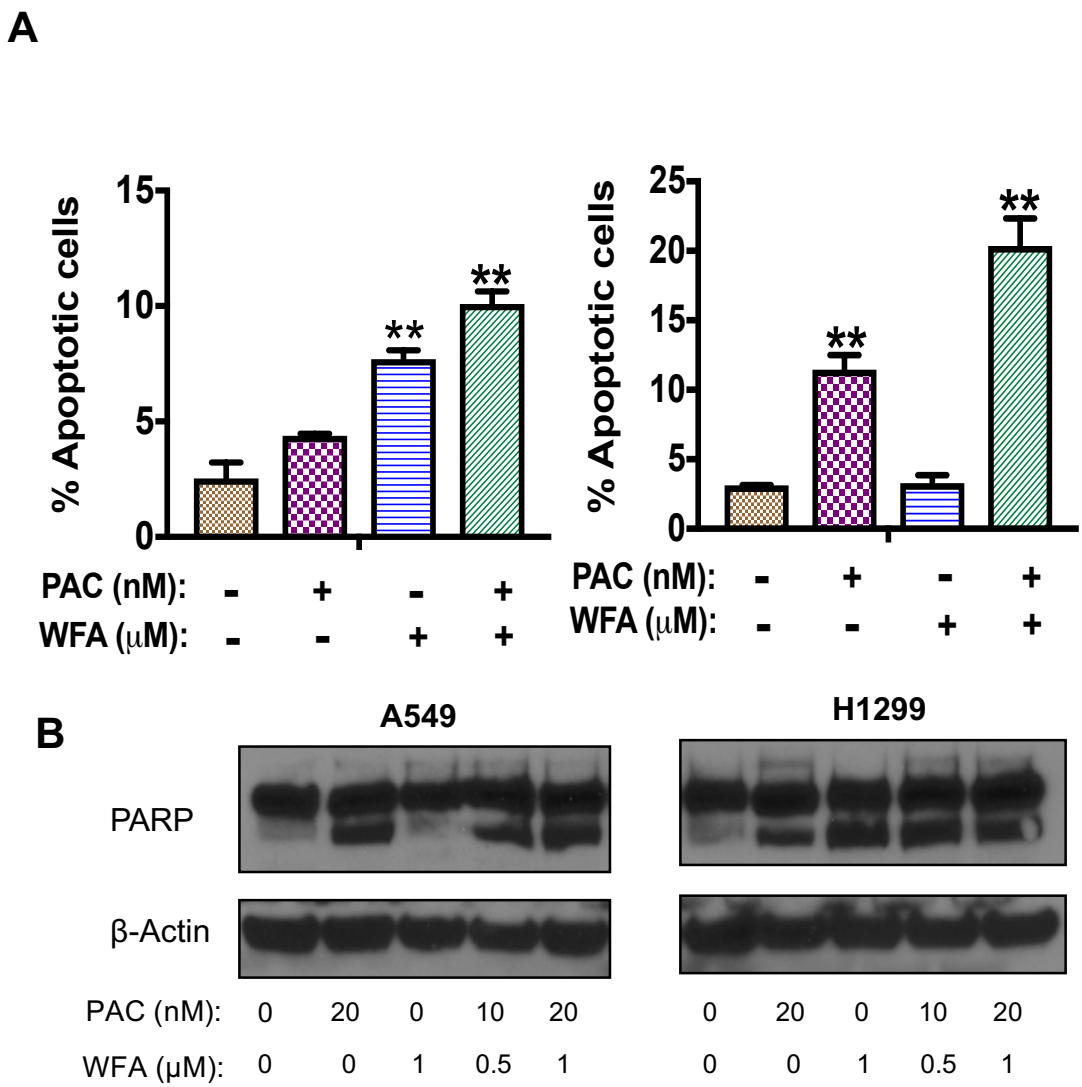

Figure 7. Effect of PAC and WFA on induction of apoptosis in H1299 and A549 NSCLC cells. (**A**). PAC and WFA increased the percentage of AnnexinV positive (apoptotic) cells compared to controls in both H1299 and A549 cells. PAC had higher activity against A549 cells while WFA had greater activity against H1299 cells. The combination of PAC and WFA had a significantly (**$p<0.05$) induced apoptosis in a higher percentage cells than either PAC or WFA alone (**B**) Western blot analysis of whole cell lysates after incubation with PAC and WFA alone, and in combination indicating increased levels of cleaved-PARP.

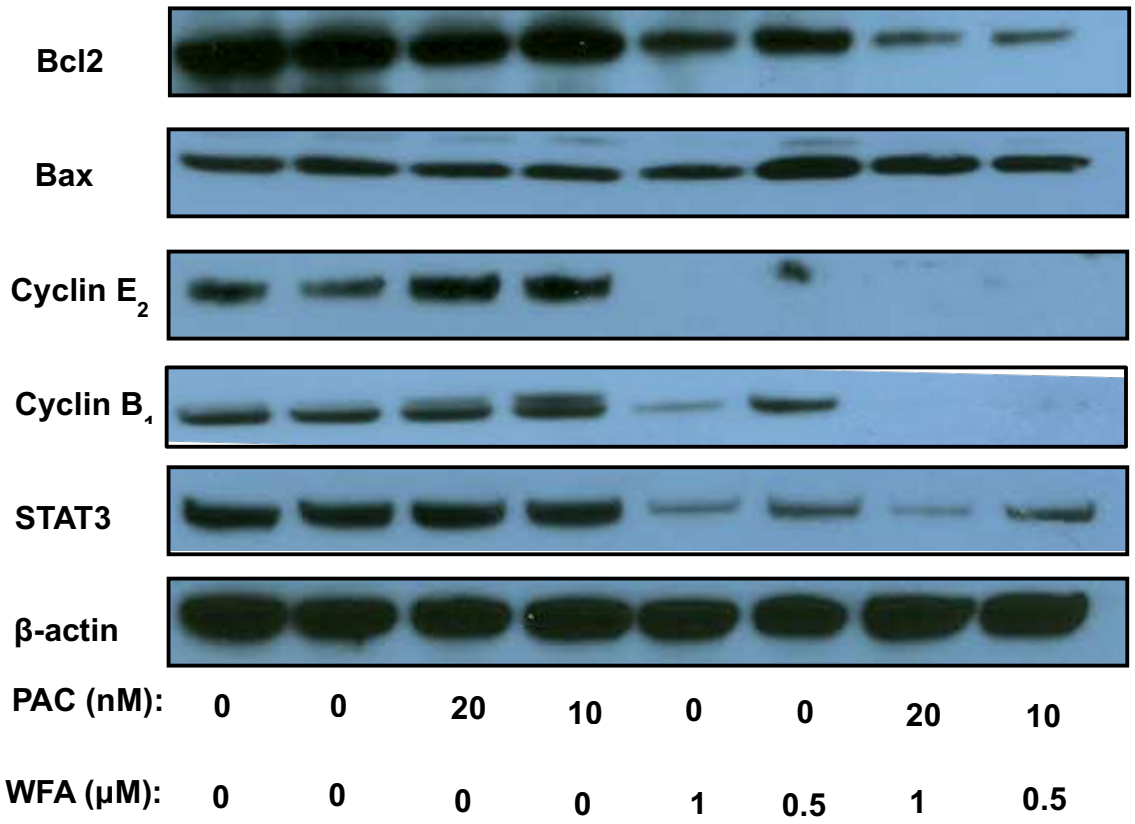

Figure 8. Western blot analysis depicting the effect of PAC and WFA alone and in combination on regulators of apoptosis and cell cycle. PAC alone had minimal inhibitory effects on the expression of the mitochondrial anti-apoptotic protein Bcl-2, but WFA had a dose-dependent inhibition of Bcl-2 expression. The combination of PAC and WFA significantly decreased the levels of Bcl-2 than either PAC or WFA alone, indicating greater pro-apoptotic potential. Furthermore, the levels of the pro-apoptotic protein Bax were minimally affected by PAC alone but increased in response to WFA alone or in combination with PAC. The cell cycle regulatory proteins Cyclin E_2, Cyclin B_1 and STAT3 were also minimally affected by PAC compared to controls but were decreased when cells were incubated with WFA alone and in combination with PAC. β-actin was used as total protein loading control.

Effect of PAC and WFA on the migration of H1299 and A549 cells.

The migratory capacity of NSCLC cells is a key molecular event in the ability of primary tumors to establish distant metastases. Therefore, we investigated the anti-migratory effects of PAC and WFA alone and in combination against H1299 and A549 cells. The wound healing assay was performed and used to determine the rate of migration or motility of both H1299 or A549 cells over 24 hours in the presence of PAC (10 nM) or WFA (0.5 μM) alone and in combination.

Figure 9 shows the migration of H1299 cells over a 24-hour experimental in cell culture. The results indicate that H1299 cells cultured in DMEM alone (vehicle) achieved almost 100% migration into the cell gap at 24 hours. In the presence of PAC alone, a minimal effect on H1299 cell migration (>80% migration) compared to the migration in control wells was observed. In contrast, in the presence of WFA, there was a statistically significant (*$p<0.05$) inhibitory effect on cell migration (<70% migration). Furthermore, when cells were incubated with the combination of PAC and WFA, the anti-migratory effects were dramatically enhanced and even greater inhibition (#$p<0.05$ versus WFA alone) of H1299 cell migration (<50% migration). Figure 10 shows the wound healing assay for the migration of A549 cells depicting up to 50% and 60% inhibition of A549 cell migration for PAC and WFA, respectively. As was observed for H1299 cells, the combination of PAC and WFA had a significantly (#$p<0.05$ versus WFA) greater inhibitory effects on the migratory capacity of both H1299 and A549 NSCLC cells compared to either PAC or WFA alone.

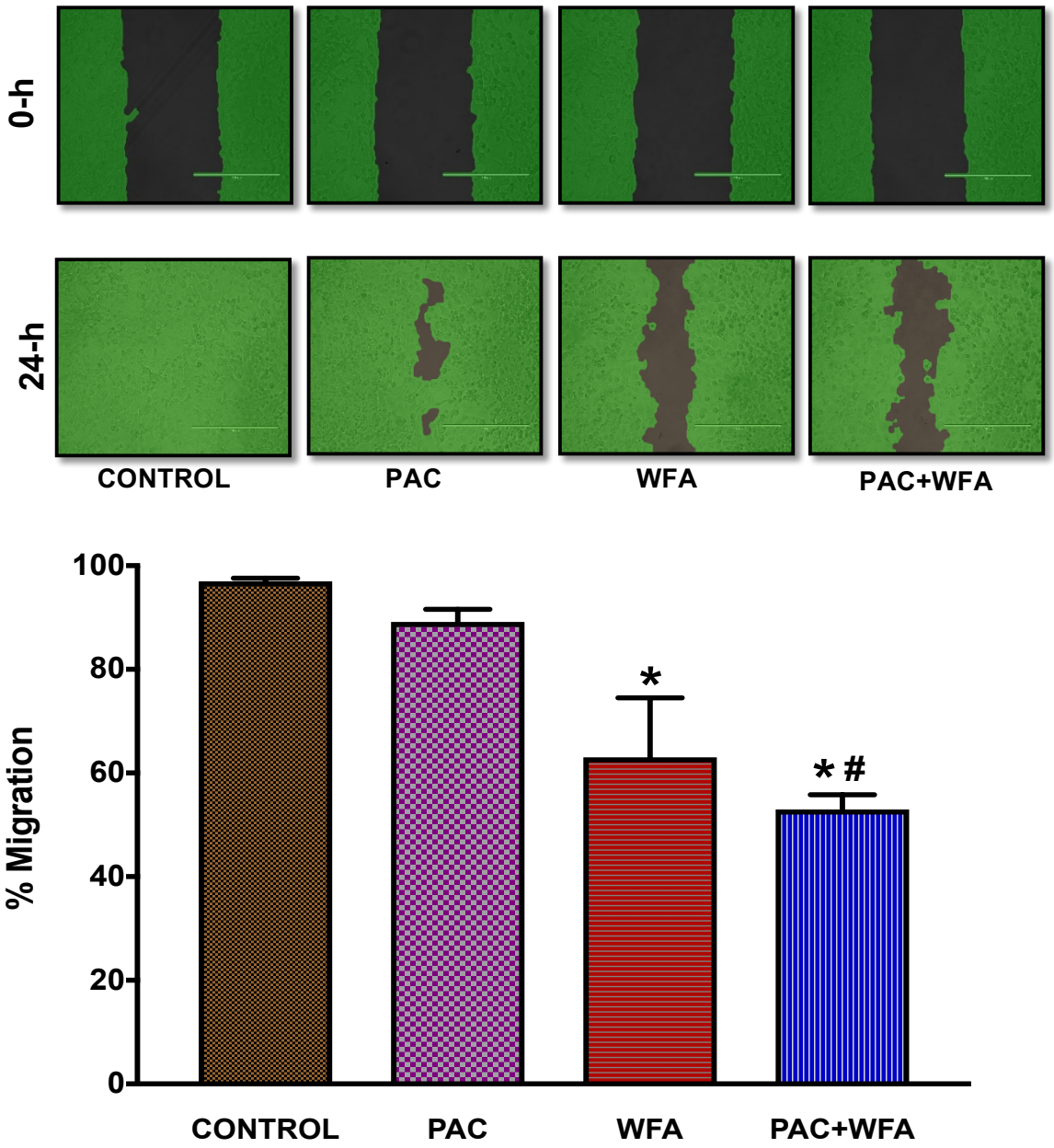

Figure 9. Wound healing assay depicting migration of H1299 NSCLC cells. The area covered with cells is indicated in green and was compared between time 0 and 24 h to determine percent migration. The control group of cells, cultured in media alone had increased migratory capacity (>99%) within 24 hours. PAC (10 nM) had minimal effect on H1299 cell migration (80-90% migration) which was not statistically significant. However, incubation of cells with WFA (0.5 μM) alone significantly (*$p<0.05$) inhibited the cell migration compared to control. Further, H1299 cells incubated in media containing a combination of PAC and WFA (1:50) significantly inhibited the migration of cells in the gap area greater than either PAC or WFA alone (*$p<0.05$ versus control, and #$p<0.05$ versus either PAC of WFA alone). Data are mean±SD of 3 experiments.

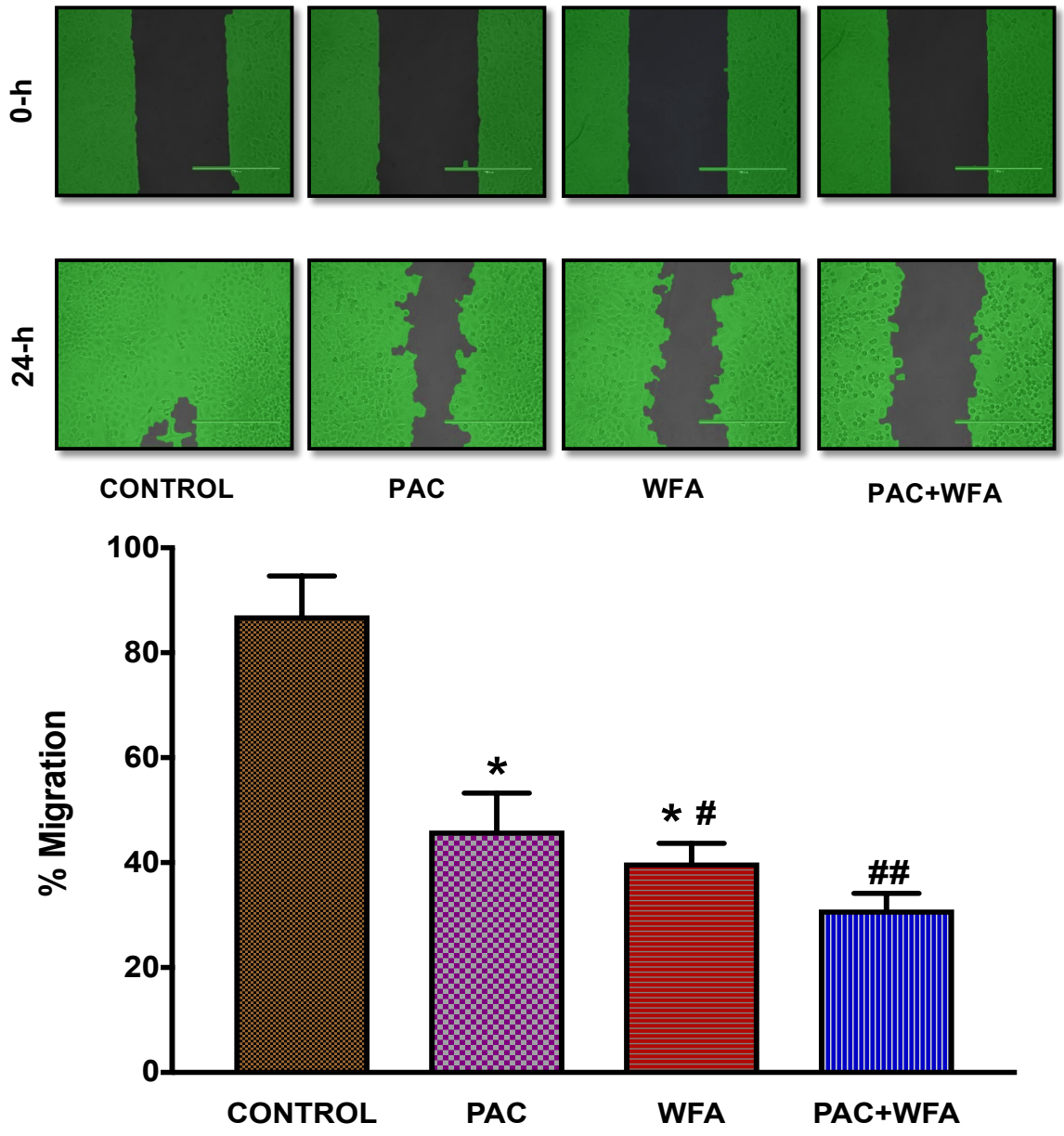

Figure 10. Wound healing assay depicting migration of A549 NSCLC cells. The area covered with cells is indicated in green and was compared between time 0 and 24 h to determine percent migration. The control group of cells, cultured in media alone had increased migratory capacity (80-95%) within 24 hours. A549 cells incubated with PAC (10 nM) alone had decreased percent migration (<60%) which were statistically significant (*$p<0.05$) compared to control group of cells. Further, WFA (0.5 μM) alone significantly (*$p<0.05$ versus control, #$p<0.05$ versus PAC alone) inhibited A549 cell migration. The combination of PAC and WFA (1:50) resulted into much lower percent migration (<40%) that was statistically significant compared to either PAC or WFA alone (##$p<0.05$ versus either PAC of WFA alone). Data are mean±SD of 3 experiments.

Effect of PAC and WFA on TGFβ1-induced EMT in H1299 and A549 cells

Epithelial-to-mesenchymal transition (EMT) is set of complex cellular events which cancer cells undergo to transition from an epithelial to a mesenchymal phenotype. This process enhances the migratory capacity of cells and increases the chance of metastasis. To investigate whether WFA alone or in combination with PAC inhibited TGFβ1-induced EMT in H1299 and A549 cells, we compared the cellular morphology and the expression levels of known molecular markers of mesenchyme phenotype between cells cultured with PAC and WFA, alone and the combination.

Figure 11 shows that A549 cells cultured in serum-free media had visible cell-cell contact, and a rounded cell shape typical for that cell line. However, the incubation of these cells with 5 ng/mL TGFβ1 in serum-free media, cells caused significant changes in cell morphology characteristic of the transition from an epithelial to mesenchymal phenotype. To corroborate these findings, western blot analysis (Figure 12) of whole-cell lysates of A549 and H1299 cells following incubation with 5 ng/mL of TGFβ1 with or without PAC or WFA alone and in combination was performed. The results indicate that TGFβ1 induced the expression of EMT markers, vimentin, β-catenin, Snail, and ZEB while decreasing the levels of the epithelial marker E-cadherin in either A549 or H1299 cells. Together, the morphology changes and EMT protein expression was considered a positive change of the cells from an epithelial to mesenchymal phenotype. For both cell lines, PAC had minimal effects on the TGFβ-induced EMT markers within the experimental period of 24 hours. In contrast, in the presence of WFA alone,

there was significant inhibition of the expression of EMT markers in both cell lines. There was a dose-dependent inhibition of vimentin, β-catenin, Snail, and ZEB expression when cells were incubated with WFA alongside TGFβ1. Furthermore, for both NSCLC cell lines, the observed TGFβ1-induced downregulation of E-cadherin was also inhibited when cells were incubated in the presence of WFA. The combination of PAC and WFA had an even greater inhibitory effect on TGFβ-1 induced EMT in A549 and H1299 cells. Based on these findings, we explored the ability of PAC and WFA to inhibit adhesion and migration induced by TGFβ1.

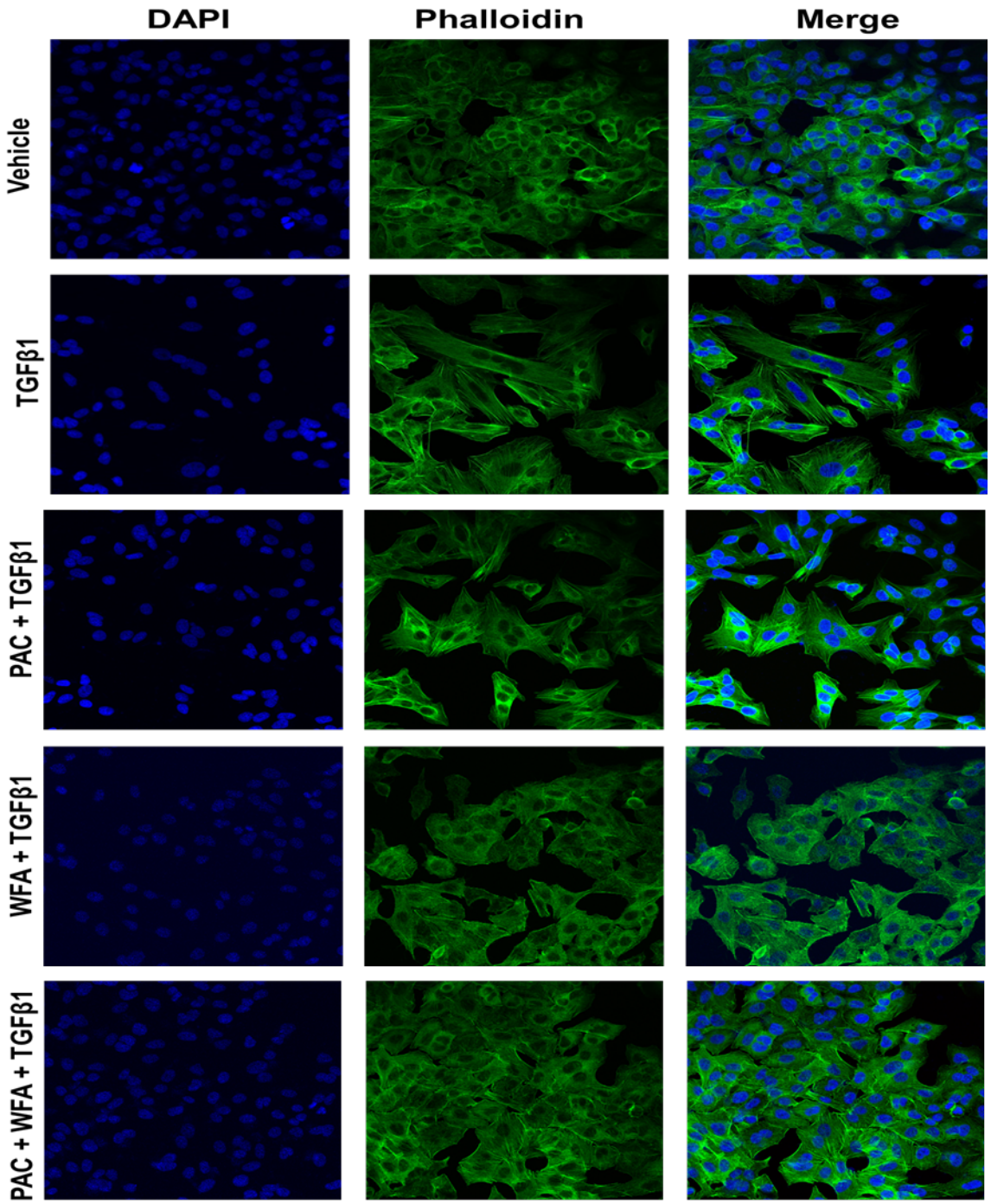

Figure 11. Immunofluorescence staining depicting the effect of PAC and WFA on TGFβ1-induced morphological changes in A549 cells. Cells were cultured in 8-well μ-slides, serum starved for 24 prior to the treatment and incubated with 5 ng/mL TGFβ1 in serum-free media for an additional 24 hours. WFA alone, and in combination with PAC inhibited the morphological changes induced by TGFβ1.

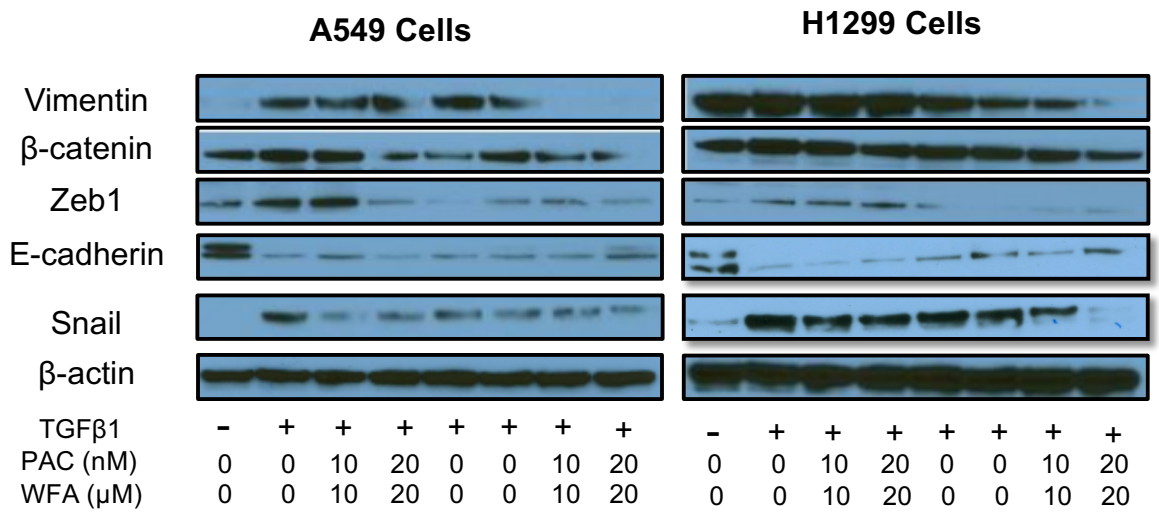

Figure 12. Western-blot analysis depicting the effect of PAC and WFA on TGFβ1-induced EMT in A549 cells cultured for 24 hours. Cells cultured in serum-free media alone had minimal expression of EMT markers. However, A549 and H1299 cells cultured in serum-free media containing TGFβ1 (5 ng/mL) had an increased expression of EMT protein markers, vimentin, and β-catenin as well as transcription factors ZEB and Snail but decreased levels of the protein E-Cadherin. WFA, alone and in combination with PAC, inhibited the TGFβ1-induced EMT in both cell types. β-actin was used as an internal loading control.

Effect of PAC and WFA on TGFβ1-induced adhesion of H1299 and A549 cells

Cell adhesion refers to the ability of cells to bind to an extracellular matrix or other cells. This process involves complex biochemical changes in the cells that result in the expression of specific molecules on the surface of the cell and it is important for cell-cell communication, growth, and survival of cells. Through cell adhesion, circulating tumor cells can establish distant metastases by attaching to distant tissues. Therefore, we investigated whether WFA and PAC alone and in combination could inhibit TGFβ1-induced adhesion of H1299 and A549 cells.

Figures 13 and 14 show the findings from the cell adhesion assay for A549 and H1299 cells, respectively. In each case, the OD values from cells cultured in serum-free media were presented as 100% cell viability and used as a reference to calculate the fold change in adhesion when cells were cultured in serum-free media containing TGFβ1. In figure 12, A549 cells cultured in serum free media containing 5 ng/mL of TGFβ1 had significantly (*$p < 0.05$) higher (4-fold) percent adhesion to matrigel compared to A549 cells cultured in serum-free media alone (control). However, when A549 cells were incubated with TGFβ1 in the presence of PAC [12-100 nM] alone, there was a dose-dependent decrease in percent cell adhesion compared to cells that were cultured with TGFβ1 alone (**$p<0.05$ for PAC+TGFβ1 versus TGFβ1). Similarly, A549 cells seeded in media containing TGFβ1 and WFA [0.6-5.0 nM] alone had a statistically significant (**$p<0.05$ for WFA+TGFβ1 versus TGFβ1) dose-dependent reduction in percent cell adhesion compared to cells cultured in the presence of TGFβ1 alone. However, when PAC and WFA were combined (at 1:50 ratio, respectively), the dose-dependent

decrease in percent A549 cell adhesion was significantly enhanced than when either PAC or WFA when used alone.

Figure 14 shows the results of the cell adhesion assay depicting the inhibitory effects of PAC or WFA alone and in combination against TGFβ1-induced H1299 cell adhesion. As was the case for A549 cells in figure 13, the viability of H1299 cells cultured in serum-free media was considered as 100% adhesion. When H1299 cells were incubated in serum-free media containing 5 ng/mL of TGFβ, there was a 2-fold increase in H1299 cell adhesion compared to H1299 cells that were incubated in serum free media without TGFβ1. Further, both PAC and WFA alone had statistically significant (**$p<0.05$) dose-dependent inhibitory effects on H1299 cell adhesion induced by TGFβ1. Interestingly, at the indicated concentrations, WFA alone had a greater inhibitory effect on cell adhesion than PAC alone but the combination of the two had greater inhibitory effects on cell adhesion than the individual agents alone. Together, these data suggest that combination of PAC and WFA can significantly inhibit adhesion of NSCLC cells to matrigel *in vitro* which suggests the ability to inhibit metastasis *in vivo*.

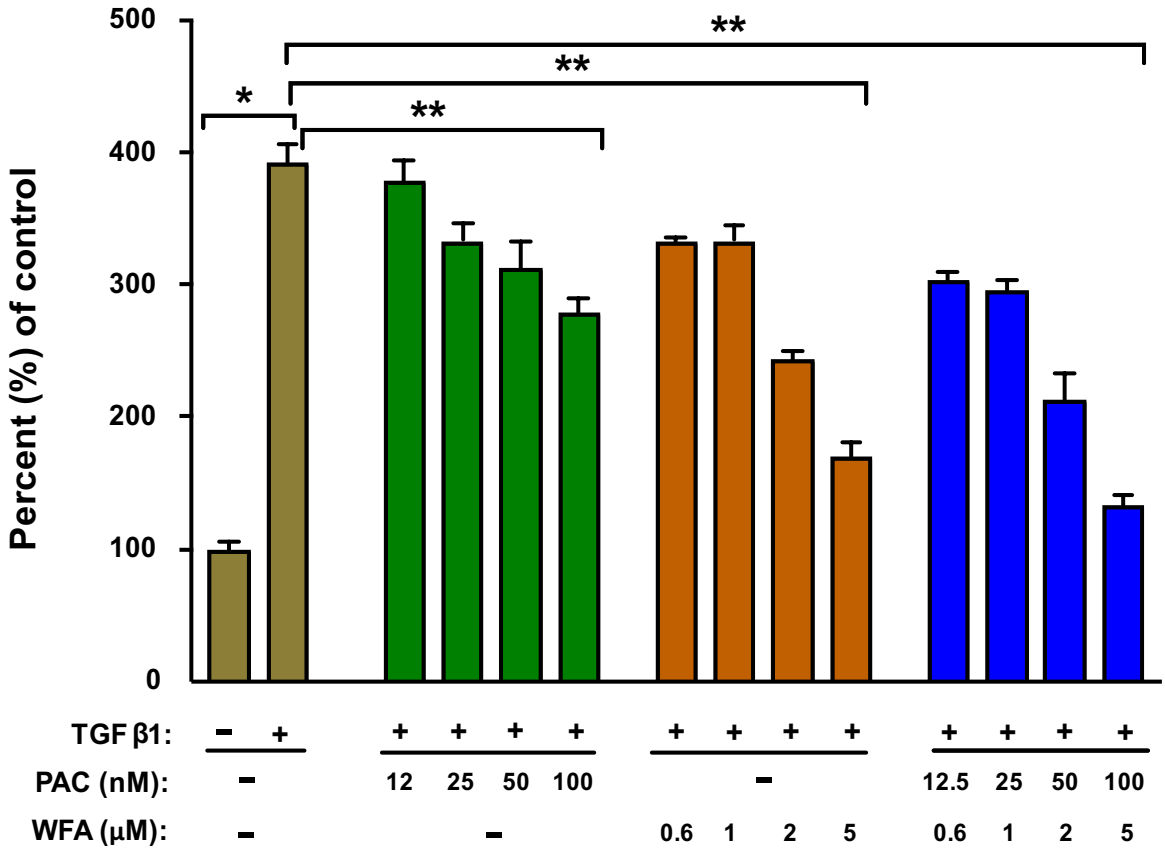

Figure 13. Effect of PAC and WFA, alone and in combination, on TGFβ1-induced adhesion of A549 NSCLC cells to matrigel. The figure shows that TGFβ1 (5 ng/mL) significantly (*p<0.05) increased the adhesion of A549 (4-fold) compared to cells cultured in serum-free media alone (control). However, either PAC or WFA alone had a statistically significant dose-dependent inhibitory effect (WFA>PAC) on TGFβ1-induced adhesion of A549 cells to matrigel (**p<0.05 compared to TGFβ1 alone). The combination of PAC and WFA had an even greater inhibitory effect on TGFβ1-induced adhesion of cells than either PAC or WFA alone. Data are percent (Mean ± SD) of controls.

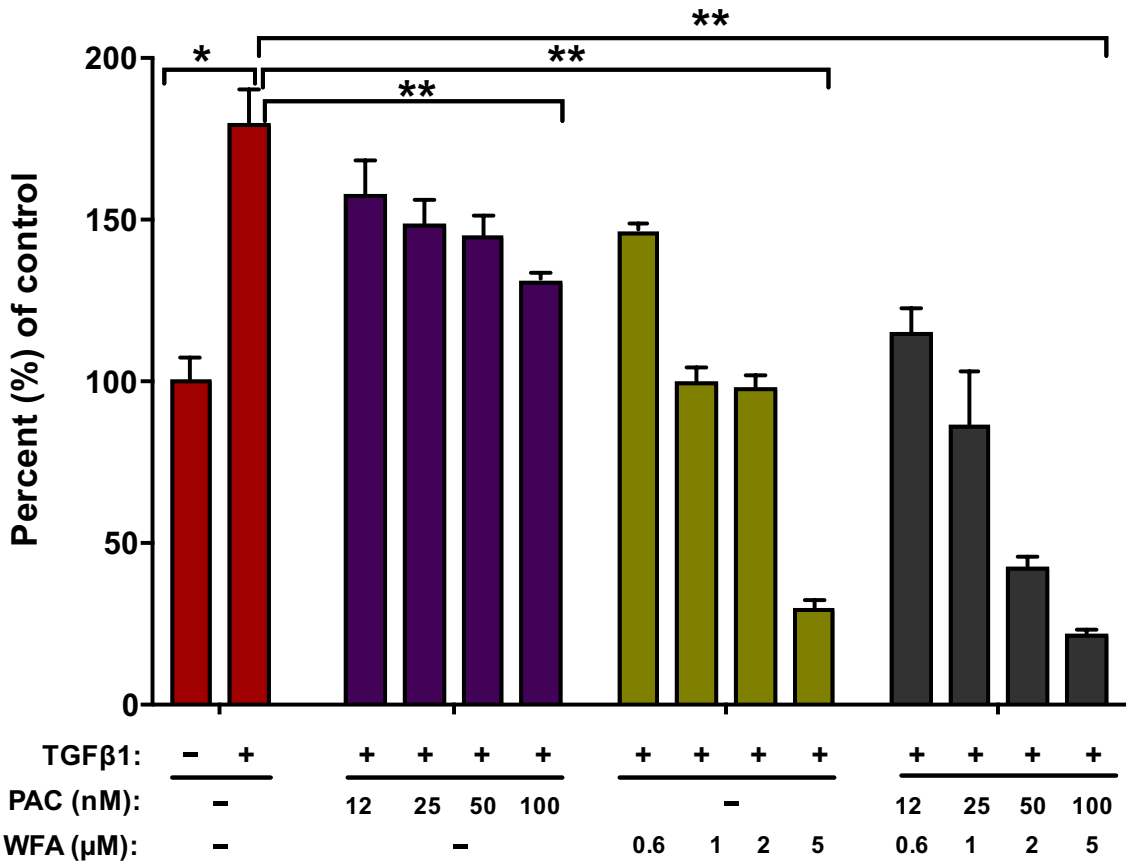

Figure 14. Effect of PAC and WFA, alone and in combination, on TGFβ1-induced adhesion of H1299 NSCLC cells to matrigel. The figure shows that TGFβ1 (5 ng/mL) significantly (*p<0.05) increased the adhesion of H1299 cells (2-fold) compared to cells cultured in serum-free media alone (control). In contrast, either PAC or WFA alone had a statistically significant dose-dependent inhibitory effect (WFA>PAC) on TGFβ1-induced adhesion of H1299 cells to matrigel (**p<0.05 compared to TGFβ1 alone). The combination of PAC and WFA had an even greater inhibitory effect on TGFβ1-induced adhesion of cells than either PAC or WFA alone. Data are percent (Mean ± SD) of controls.

Effect of PAC and WFA on TGFβ1-induced migration of H1299 and A549 cells

The objective of this study was to determine whether WFA or PAC alone or in combination could inhibit TGFβ1-induced migration of A549 and H1299 NSCLC cells. The wound healing assay was performed to mimic the *in vitro* migration of H1299 and A549 cells using cell culture inserts in serum-free media. Cell motility was monitored using a microscope at 0 hours and at 24 hours to determine the extent of cell migration in serum free media containing 5 ng/mL of TGFβ1 in the presence of either PAC or WFA alone and in combination.

Figure 15 shows that H1299 cells cultured in serum-free media without TGFβ1 (control) had minimal migration (<5%) between 0 and 24 hours. However, in the presence of 5 ng/mL of TGFβ1, H1299 cells had significantly (*$p<0.05$) increased migratory capacity (>80%) compared to the controls within 24 hours. However, as was observed for the cell adhesion assay, PAC alone (20 nM) had a statistically significant (#$p<0.05$) inhibitory effect on TGFβ1-induced migration of H1299 cells compared to H1299 cells cultured with TGFβ1 alone. Thus, there was only 50% migration into the cell gap when H1299 cells were incubated with PAC alongside TGFβ1 in serum-free media. Similarly, in the presence of WFA (1 μM) alone, there was less than 20% migration of H1299 cells into the cell gap which was statistically significantly (#$p<0.05$) lower than H1299 cells cultured with TGFβ1 alone. When H1299 cells were cultured in media containing TGFβ1 in the presence of both PAC and WFA, the percent migration was less than 10% and statistically different from either PAC or WFA alone (##$p<0.0.001$).

Figure 16 depicts the effect of PAC or WFA alone and in combination on the migration of A549 cells induced by TGFβ1 in serum-free media. The figure shows that A549 cells cultured in serum-free media had minimal migration (10-20%) between 0 and 24 hours. As was observed with H1299 cells in figure 14, by co-treatment, PAC alone significantly inhibited the TGFβ1-induced migration of A549 cells. Furthermore, WFA alone also inhibited TGFβ1-induced cell migration of A549 but with greater efficacy than PAC. However, the combination of PAC and WFA had significantly lower percent (<5%) migration of A549 cells than either PAC or WFA alone, indicating much greater inhibition of cell motility. Together, these findings indicated that both PAC and WFA alone had inhibitory effects on H1299 and A549 migration induced by TGFβ1 in serum-free media and that the inhibitory effects were enhanced when PAC was used together with WFA.

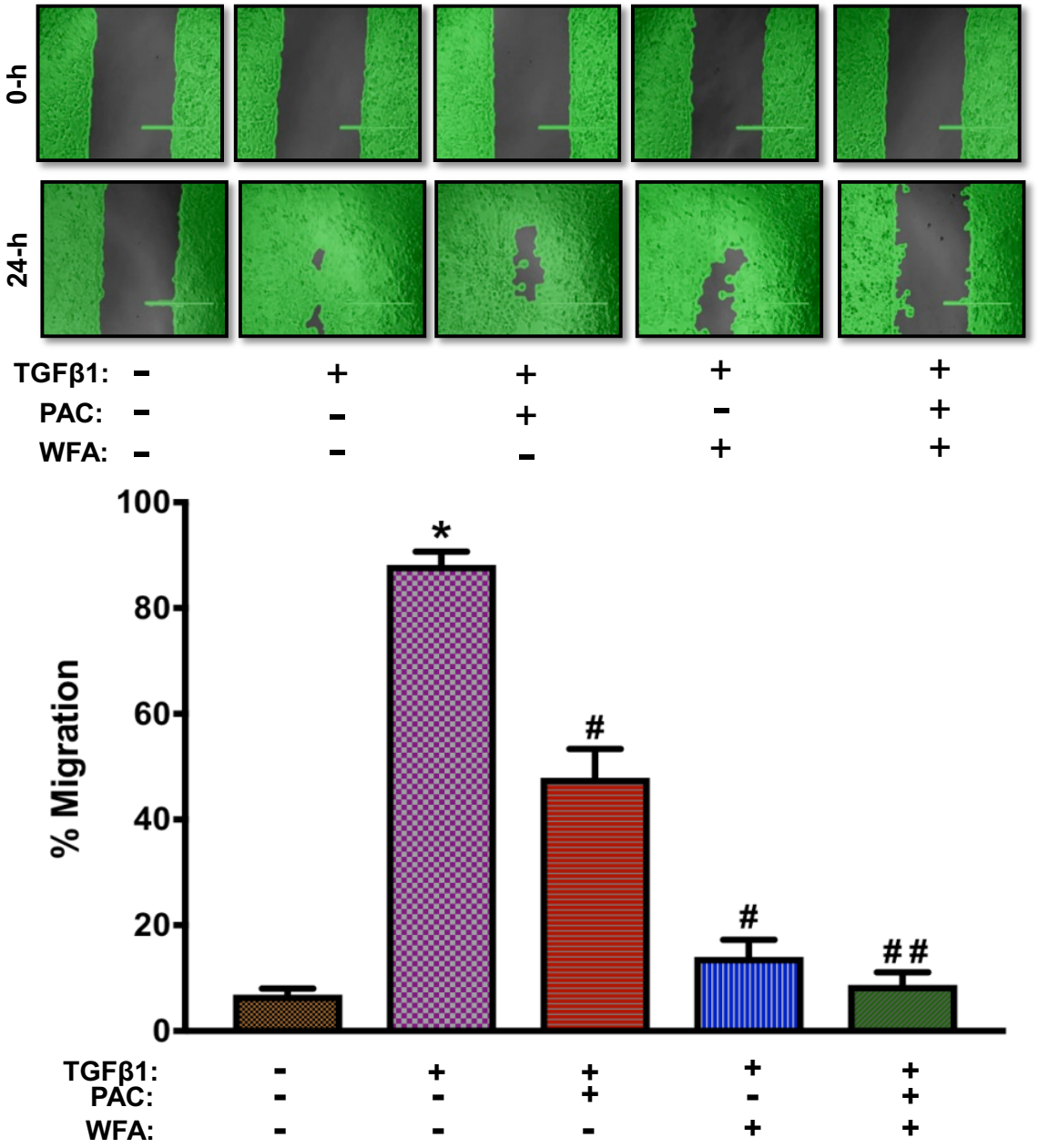

Figure 15. Inhibition of TGF-β1-induced migration in H1299 cells. The figure depicts minimal migration of H1299 cells cultured in serum-free media. However, TGF-β1 (5 ng/mL) in serum-free media increased the migration of H1299 cells into the scratch area within 24-hours (**p<0.05). Also, PAC (10 nM) and WFA (0.5 μM) significantly inhibited (WFA>PAC) the TGF-β1-induced migration of H1299 cells (## p<0.05 vs TGFβ1). The PAC and WFA had a greater inhibitory effect induced migration of A549 cells in vitro than each agent alone (### p<0.001 vs. PAC and WFA alone).

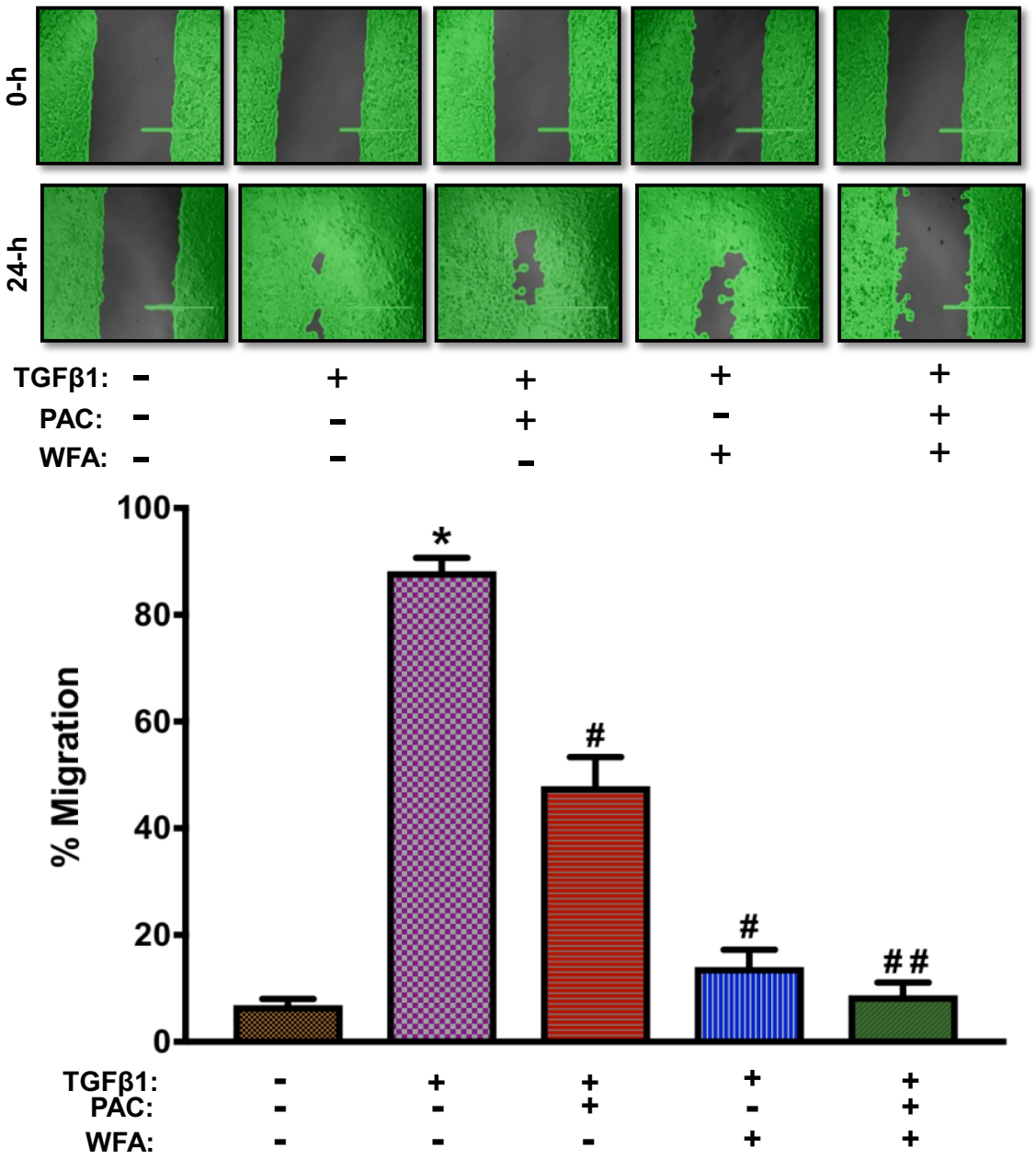

Figure 16. Inhibition of TGF-β1-induced migration in A549 cells. The figure depicts minimal migration of A549 cells cultured in serum-free media. Incubation of cells with TGF-β1 (5 ng/mL) in serum-free media increased the migratory capacity into the scratch area within 24-hours (**p<0.05). PAC (10 nM) and WFA (0.5 μM) significantly inhibited (WFA>PAC) the TGF-β1 induced migration (## p<0.05 vs. TGFβ1). The c of PAC and WFA had a greater inhibitory effect on TGF-β1-induced migration of A549 cells *in vitro* than each agent alone (### p<0.001 vs. PAC and WFA alone).

Effect of PAC and WFA on TGFβ1-induced transwell migration and invasion of H1299 and A549 cells

The objective of this study was to determine whether PAC or WFA alone and in combination inhibited the migration of H1299 or A549 cells from the upper to bottom chamber in a transwell plate. Cells were cultured in serum-free media in the upper chamber and media containing serum was placed at the bottom as a chemoattractant. The results are presented as microphotographs of migrated cells at the bottom of the transwell plate stained with toluidine blue dye after 24 hours.

Figure 17 shows the results of the transwell migration assay while figure 18 shows findings from the matrigel invasion assay. Here, the migration assay indicated that both A549 and H1299 cells, when cultured in serum-free media, had minimal migration to bottom chamber of the transwell plates. However, in the presence of TGFβ1, there was a remarkable and statistically significant increase in the number of cells that migrated. When cells were co-cultured with TGFβ1 and PAC alone, there was a decrease in the number of migrated cells when compared to TGFβ1 alone. The effect of PAC alone on TGFβ1-induced migration was greater for A549 cells than was observed in H1299 cells. Similarly, when H1299 or A549 cells were cultured with TGFβ1 and WFA alone, there was a significant decrease in the number of cells that migrated to the bottom of the transwell plate. Interestingly, unlike what was observed with PAC, the effect of WFA was more pronounced against H1299 than A549 cells. As was observed with other assays, the combination of WFA and PAC had much greater inhibition of TGFβ1-induced migration of either H1299 or A549 cells compared with each agent alone.

Figure 18 shows the findings from the *in vitro* invasion of matrigel assay, a widely-used method to determine the anti-invasive activity of anticancer agents. Here, it was clear that serum-starved H1299 or A549 NSCLC cells cultured in serum-free media had minimal invasion as indicated by the lower number of stained cells at the bottom of the transwell chamber. However, the invasion of both cell lines was greatly increased in the presence of 5 ng/mL of TGFβ1 in serum-free media. As was observed with the transwell migration assay, similar effects of PAC and WFA alone, when co-cultures alongside TGFβ1 significantly decreased the invasiveness of cells. Further, that the combination of PAC and WFA had a significantly higher inhibitory effect on cell invasion than when both agents were used alone. Together, the findings presented from these two assays provided credence to our hypothesis that PAC and WFA, when used in combination would produce significantly greater inhibition of migration and invasion of NSCLC cells.

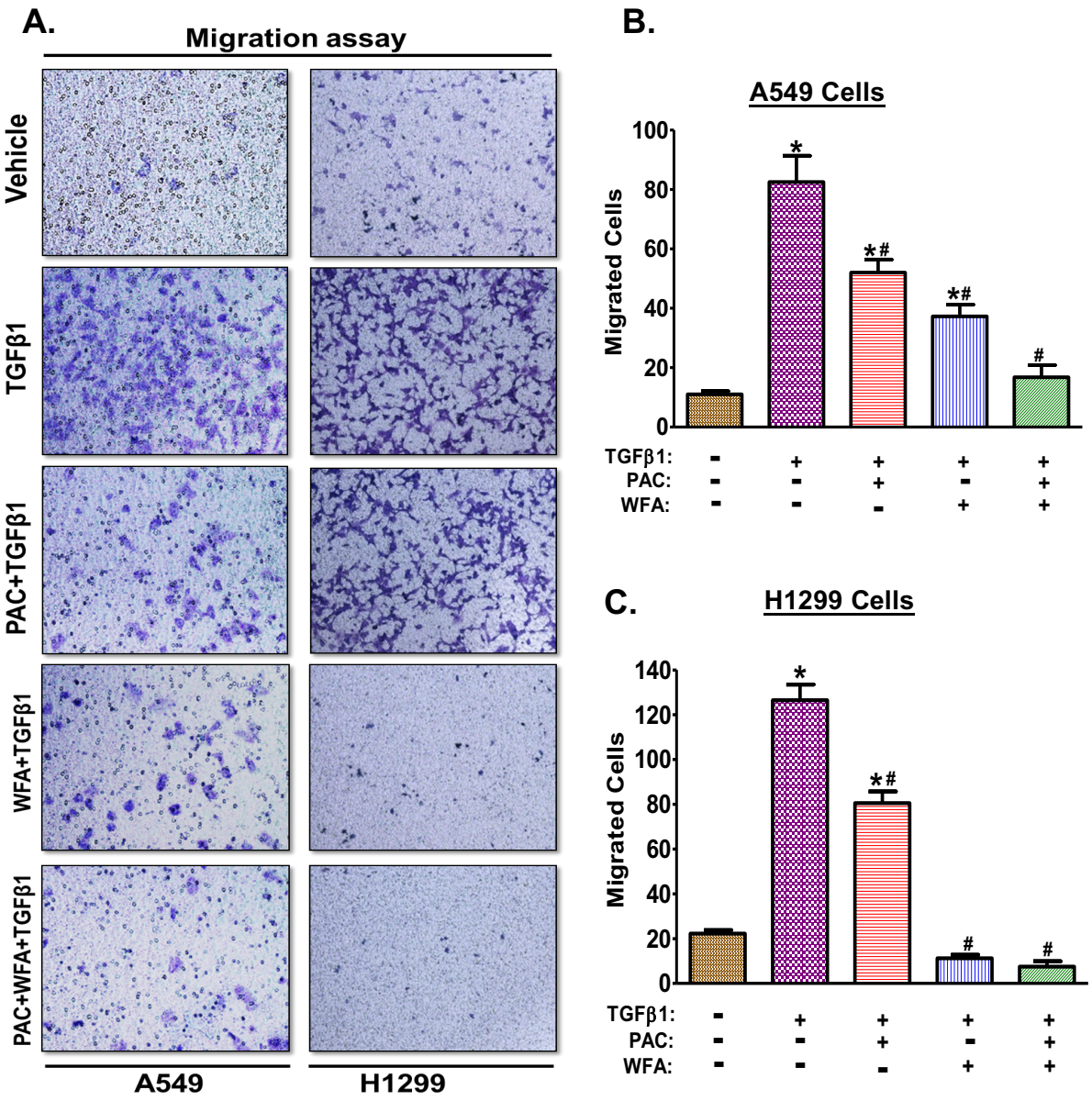

Figure 17. Inhibitory effects of PAC and WFA, alone and in combination, on TGF-β1-induced trans-well migration of A549 and H1299 cells. In control wells, cells grown in serum-free media had minimal migratory. However, TGFβ1 (5 ng/mL) significantly (*p<0.05) increased the migration of both A549 and H1299 cells. Further, PAC (20 nM) alone had a statistically significant inhibitory effect on TGFβ1-induced migration (#p<0.05 vs TGFβ1), but still greater than vehicle (*p<0.05 vs vehicle). However, WFA (1 μM) alone and in combination with PAC (20 nM) significantly decreased the number of migratory cells for both A549 and H1299 cell lines compared to TGFβ1 (#p<0.05) and the vehicle control. Data are means ±SD for each group from 3 independent experiments.

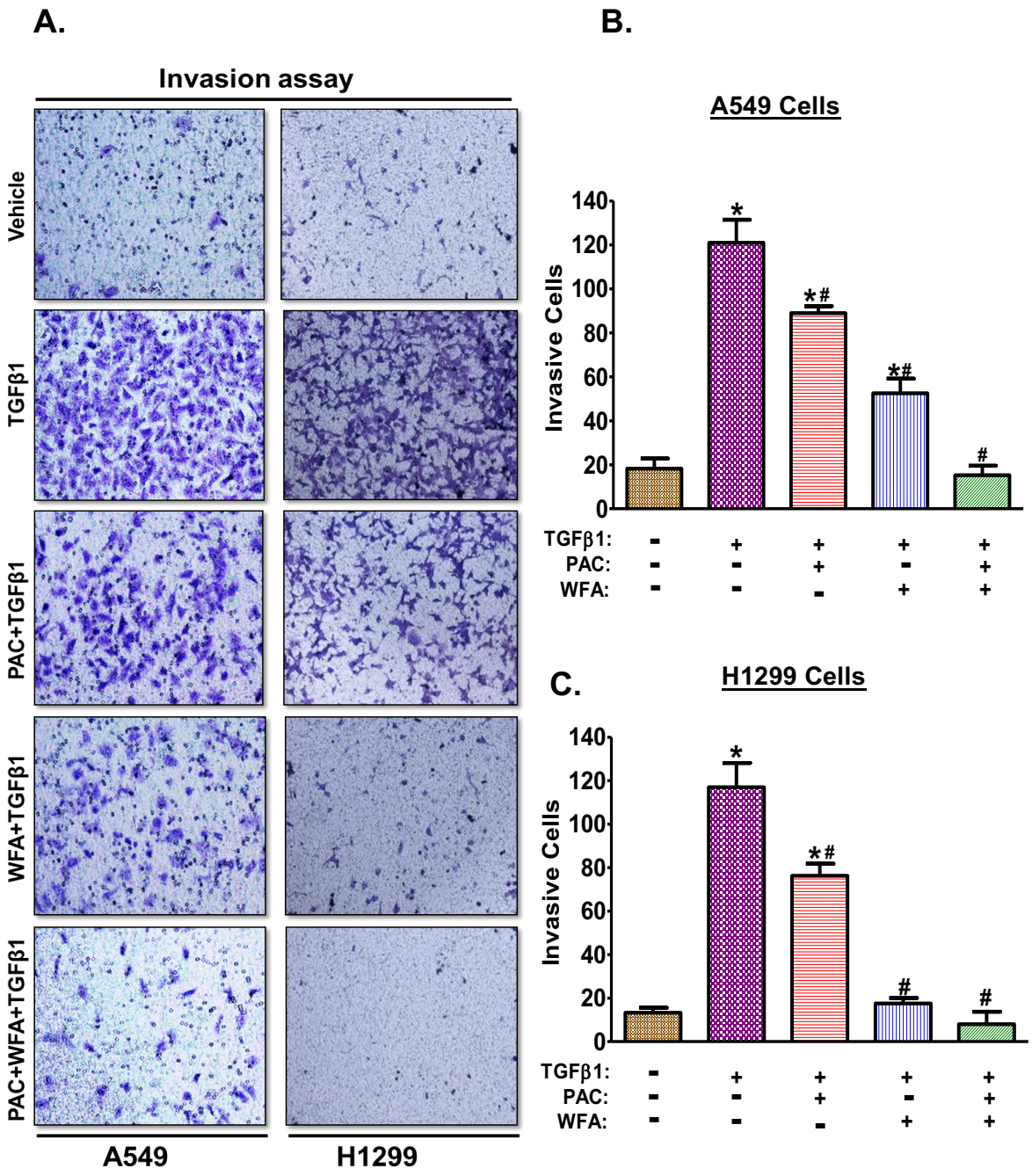

Figure 18. The inhibitory effects of PAC and WFA, alone and in combination, on TGF-β1-induced Matrigel base membrane invasion of A549 and H1299 cells. Either A549 or H1299 cells grown in serum-free media (vehicle) had a minimal number of invasive cells. Incubation of cells with TGFβ1 (5 ng/mL) significantly (*$p<0.05$) increased the invasion of both A549 and H1299 cells. PAC (20 nM) alone had a inhibited the invasion of cells in response to TGFβ1 (#$p<0.05$ vs TGFβ1. Similarly, WFA (1 μM) alone inhibited (much greater than PAC) the invasive capacity of either A549 or H1299 cells induced by TGFβ1. The combination of WFA and PAC also significantly decreased the number of migratory cells but not much greater than WFA alone. Data are means ±SD for each group from 3 independent experiments.

DISCUSSION

Lung cancer remains the leading cause of cancer-related deaths among both men and women in the U.S and worldwide [1, 2, 7]. Currently, the overall 5-year survival rate for all stages hovers around 17% while it is only 4% for those who are diagnosed with advanced disease [1, 3]. Despite improvements in imaging and diagnostic techniques as well as recent advances in chemotherapy, the prognosis of lung cancer has remained extremely poor. To date, 60- 70% of lung cancer patients are diagnosed when the tumors are at advanced stages [2]. For such patients, the tumors are not amenable to curative surgery due to metastasis, and the therapeutic objective is not to cure but to manage symptoms and prolong the lives of patients [13, 18, 23]. Therefore, chemotherapy, targeted or immunotherapy alone or in combination are the cornerstone of lung cancer treatment [12, 23].

Currently, several drugs are approved for the treatment of advanced NSCLC but the platinum drugs (either carboplatin or cisplatin) in combination with PAC are the most widely used as first-line regimens [6]. PAC or taxol, a member of the taxanes was first approved by FDA for the treatment of NSCLC in 1999 [64]. Mechanistically, PAC acts by binding to β-tubulin and stabilizing microtubules during cell division causing mitotic arrest [64]. Whether cells undergo apoptosis or not following mitotic arrest by PAC is dependent on efficient mitotic checkpoint mechanisms which are often dysregulated in NSCLC cells. Consequently, the

the response rate of NSCLC to the platinum drugs-PAC regimen is only up to 25% and clinical efficacy has plateaued at about 10-14 months [6, 18]. Further, the clinical efficacy of PAC is limited by its poor solubility, drug resistance and dose-limiting life-threatening toxicity [13]. To overcome the challenges with cytotoxic compounds like PAC, targeted therapies and immune checkpoint inhibitors have been developed and approved for NSCLC treatment. However, even with these drugs, it is widely reported that only 60% of NSCLC tumors show targetable mutations and only 25% of patients benefit from immunotherapy [25]. Therefore, there is an unmet need to develop safe and efficacious drugs for the treatment of advanced lung cancer.

In the present study, a novel strategy aimed at improving the clinical efficacy, delay drug resistance and decrease the toxicity of PAC against NSCLC was explored. This strategy has been explored elsewhere [28] and the effects of combining standard chemotherapeutic agents with novel non-toxic plant-derived anticancer compounds against various cancer types are being investigated. Presently, we focused on WFA because it is one of the most promising plant-derived lead anticancer compounds with the potential to become a clinically useful drug. Over the past decade or so, preclinical data has accumulated indicating the potency and efficacy of WFA against various cancer cell types. A review of the literature shows that several studies have been published demonstrating the *in vitro* and *in vivo* efficacy of WFA against the proliferation of various cancer cell types [37, 39, 65-67]. More importantly, the evidence is now accumulating indicating the potential of WFA to synergize the anticancer activity of standard

chemotherapeutic drugs like cisplatin and carboplatin against ovarian and breast cancers [40].

Building on the hypotheses from previous studies, the present study was designed to determine the effect of PAC and WFA, alone and in combination, on the proliferation, migration, and invasion of lung cancer cells. Here we demonstrated that by combining PAC and WFA, we could effectively target the proliferation of NSCLC cells and enhance the anticancer activity of PAC. The strategy of targeting cell proliferation has been reported to be a viable option for inhibiting NSCLC tumor progression and that it can provide valuable insights into the clinical efficacy of drug candidates [10]. Like the present study, several other published studies have also demonstrated the antiproliferative effects of WFA [37, 65, 68] against multiple cancer cell types. The MTT assay was used as an indirect measure of cell proliferation to demonstrate that WFA significantly enhanced the antiproliferative activity of PAC against both H1299 and A549 NSCLC cells. Comparatively, higher (>90% inhibition) antiproliferative activities of PAC were achievable by co-treatment with WFA.

From the present data, it was evident that both PAC and WFA displayed time and concentration dependent inhibition of NSCLC cell proliferation. In support of Weaver et al., [64], the median inhibitory concentrations of PAC were between 8-25 nM, concentrations which were previously reported to be clinically relevant. Furthermore, the potency of PAC was greater against A549 cells (3-fold lower IC_{50}) than was observed in H1299 cells. On the other hand, the IC_{50} values for WFA against both A549 and H1299 were in the sub-micro molar range indicating the

greater potency of PAC than WFA. Unfortunately, despite the high potency displayed by PAC compared to WFA, the overall efficacy of PAC against both cell lines was less than that for WFA. Therefore, the rationale was to combine the higher potency PAC and high efficacy WFA to achieve greater activity in the combination.

The combination strategy of PAC and WFA is justified because more than one cytotoxic drug combinations are the norm of cancer chemotherapy. However, determining synergism in a clinical scenario is not practical because it is rare to study dose-response relationships in patients. Therefore, the current *in vitr*o cell culture studies provides a useful starting point for investigating the utility of this drug combination clinically. Using the CI and fractional-effect method developed by Chou et al., [63] we demonstrated synergism between PAC and WFA against NSCLC cells. By calculating the CI values at various effect levels, the combination of PAC and WFA at constant ratios of 1:50 and 1:25 ratios displayed a synergistic (CI<1) antiproliferative activity against H1299 and A549 cells.

Like the present findings, a synergistic effect of the combination of WFA and cisplatin against ovarian cancer have been demonstrated previously [40]. In the present study, for both H1299 and A549 NSCLC cell lines, synergism (C<1) of the PAC and WFA was observed at effect levels between 25-90%. It was possible to significantly decrease the amount of either PAC or WFA required to achieve similar or higher antiproliferative activity. For example, the combination of PAC and WFA resulted in a 4-fold and a 2-fold decrease in the IC_{50} values of PAC at 1:50 and 1:25 combinatorial ratios, respectively than PAC alone. Further, it appears that the

dose reduction was dependent on the effect level and as indicated, there was greater dose reduction for PAC at 75% and 90% inhibitory effects, respectively. This dose reduction if can be validated using *in vivo* models can be exploited clinically to address the dose-limiting toxicity problems of PAC.

The synergistic effects discussed thus far were based on cell viability findings from MTT studies. Unfortunately, it is widely reported that MTT assay has major drawbacks including changes in cellular metabolic and energy processes, enzyme activity, and uptake of the MTT reagent into cells which could significantly affect the rate of metabolism of the MTT reagent. We recognized that these factors could lead to an over/underestimation of cell viability as reported by Wang *et al*., [69]. Therefore, to validate the MTT findings, the ability of PAC and WFA to induce apoptosis was also assessed. Mechanistically, the induction of apoptosis in cancer cells is the major mode of action for several cytotoxic anticancer agents [6, 16]. PAC is a potent inducer of apoptosis in many normal and cancer cell types, but, as noted earlier, the induction of apoptosis by PAC is both time and concentration dependent [64]. This is because sufficient time is required to allow effective concentrations of PAC to build up in cancer cells. Unfortunately, NSCLC cells are reported to have alternative survival pathways that enable progression of the cell cycle with poorly separated chromosomes. For this and other reasons, cytotoxic agents like PAC rarely achieve high efficacy levels at tolerable doses [6].

In the present study, PAC-induced apoptosis with greater potency in A549 cells than H1299 cells. On the other hand, WFA significantly induced apoptosis with greater potency against H1299 than A549 cells. As was observed with MTT

assay, the combination of PAC and WFA had a greater pro-apoptotic effect than either PAC or WFA alone. Interestingly, it appears that PAC and WFA induce apoptosis via distinct anticancer mechanisms making their combination viable and attractive [44]. There are two main apoptosis pathways-the extrinsic (via cell death receptors) or intrinsic (mitochondrial) pathways. Our data suggests that PAC, unlike WFA, had minimal effects on mitochondrial apoptosis regulators Bax and Bcl-2. For both compounds, there was an inhibitory effect on cell cycle regulatory proteins. Overall, these findings obtained from the apoptosis assay support the synergistic interaction of PAC and WFA and suggest that the increased antiproliferative activity of the combination was dependent on increased induction of apoptosis in both cell lines.

Metastasis remains the primary cause of death in lung cancer patients yet there are no approved drugs that specifically target this process [12]. Several published studies have indicated that mesenchymal characteristics enhance the migratory and invasive capacities of NSCLC cells during metastatic [70]. Further, that the tumor microenvironment consists of several cell types including immune cells, fibroblasts, and vascular cells which produce several factors including transforming growth factor (TGFβ1). In response to TGFβ1, NSCLC cells undergo complex biochemical changes that enable the transition of the cells from an epithelial to mesenchymal phenotype [71]. Through, EMT, cells lose cell to cell contacts, epithelial markers like E-Cadherin, and acquire mesenchymal markers like vimentin [70].

Normally, EMT is a beneficial cellular event in various physiological processes such as wound healing and embryogenesis [70], but in cancer cells, EMT is associated with cancer metastasis and resistance to chemotherapeutic agents like PAC [72]. At the molecular level, EMT is activated by signaling pathways that activate transcriptional factors like Snail, ZEB1, ZO-1, Smad2/3 and Twist [73]. Multiple lines of evidence now suggest that although TGFβ1 inhibits tumors in the early stages of carcinogenesis, it is also the most common inducer of EMT in NSCLC cells [73]. The overall result is that the EMT process increases metastatic potential of tumor cells. Therefore, we investigated whether PAC and WFA alone and in combination could inhibit the TGFβ1-induced EMT, migration, invasion and adhesion of H1299 and A549 cells.

In agreement with previous studies [62, 74], we successfully used 5 ng/mL TGFβ1 in serum-free media to induce EMT in H1299 and A549 NSCLC cells. Our findings indicate the TGFβ1 decreased the expression of E-cadherin in both A549 and H1299 cells. Also, the cells incubated with TGFβ1 alone had increased levels of vimentin, β-catenin, Snail and ZEB1. Together, the increased expression of EMT proteins coupled with repression E-cadherin was used as an indicator of a transition from an epithelial to a mesenchymal phenotype. However, in the presence of WFA alone or in combination with PAC, the expression EMT markers was inhibited. Interestingly, the inhibitory effects of WFA on TGFβ1-induced EMT were observed at sub-cytotoxic concentrations for the incubation period of 24 hours. Based on the present findings, it was not determined whether the inhibitory effects of WFA were related to decreased synthesis or increased degradation of

these specific proteins. But as per findings from previous studies conducted with breast cancer cells [39], it was hypothesized that the observed low expression levels of vimentin could be related to direct binding of WFA to vimentin and causing its degradation. Nevertheless, the mechanisms of action of WFA related to its inhibition of the expression of EMT proteins remain to be determined.

To mimic metastasis *in vitro*, the cell adhesion assay, migration and invasion assays were also performed. Cell adhesion is defined as the binding of cells to an extracellular matrix or other cells and is important for the cell to cell communication and growth. Increased cell adhesion of NSCLC can be an indicator of enhanced the ability of cells to establish distant metastases. In agreement with the findings of Wang *et al*., [62], TGFβ1 increased cell adhesion, motility, migration, and invasion of both A549 and H1299 cells. The increased adhesion of H1299 and A549 cells to matrigel in response to TGFβ1 were inhibited by either PAC or WFA alone and the combination had a much greater inhibitory effect. Similarly, the migratory and invasive capacities of H1299 and A549 cells were increased by TGFβ1. Together, the findings from these assays demonstrate the potential of WFA alone and in combination with PAC as an anti-metastatic regimen for NSCLC.

Therefore, the presented data indicates that PAC and WFA not only inhibited NSCLC cell proliferation but also inhibited their migration, invasion and cell adhesion. Moreover, the inhibitory effects of the two agents in combination were found to be synergistic. As preliminary findings, the current results highlight the potential of the PAC-WFA combination against NSCLC in humans. However, there is need to replicate the experiments in appropriate animals models.

SUMMARY AND CONCLUSIONS

PAC alongside platinum-based drugs is the mainstay for advanced NSCLC because these tumors are not amenable to curative surgery due to metastasis. However, this treatment regimen has reached the plateau of clinical efficacy due to organ toxicity, drug resistance, efficacy and solubility problems. In the present study, we explored a simple but effective strategy of combining WFA, a novel plant-derived anticancer with PAC to increase efficacy and decrease toxicity. The results presented here demonstrate that WFA synergistically interacted with PAC to inhibit the proliferation, cell adhesion, migration and invasion of H1299 and A549 NSCLC cells. Although PAC displayed higher potency than WFA, the overall efficacy was lower than that of WFA against either H1299 or A549 cells. However, when PAC and WFA were combined, the potency and efficacy of the combination were enhanced and significant dose reductions for PAC and WFA were achieved. The observed synergistic antiproliferative effects of PAC and WFA were attributed to increased induction of apoptosis in both H1299 and A549 cells. Furthermore, the synergism displayed here by the combination of PAC and WFA may be explained in part, because the two agents are known to act via distinct mechanisms. In conclusion, present data demonstrates the potential of WFA alone and in combination with PAC against NSCLC. Therefore, there is great promise of clinical efficacy that can be explored for advanced metastatic NSCLC.

REFERENCES

1. Siegel, R.L., K.D. Miller, and A. Jemal, *Cancer statistics, 2016.* CA: A Cancer Journal for Clinicians, 2016. **66**(1): p. 7-30.
2. Ruchalski, K.L. and K. Brown, *Lung Cancer Screening Update.* Journal of Thoracic Imaging, 2016. **31**(4): p. 190-200.
3. ACS, *Cancer facts&figures 2015. Report No.: 500815. Available from: http://www.cancer.org/acs/groups/content/@editorial/documents/document/acspc-044552.pdf.* 2015.
4. Daga, A., et al., *Current drugs and drug targets in non-small cell lung cancer: limitations and opportunities.* Asian Pac J Cancer Prev, 2015. **16**(10): p. 4147-56.
5. Herbst, R.S., J.V. Heymach, and S.M. Lippman, *Lung Cancer.* New England Journal of Medicine, 2008. **359**(13): p. 1367-1380.
6. Cufer, T. and L. Knez, *Update on systemic therapy of advanced non-small-cell lung cancer.* Expert Rev Anticancer Ther, 2014. **14**(10): p. 1189-203.
7. Spira, A., B. Halmos, and C.A. Powell, *Update in Lung Cancer 2014.* Am J Respir Crit Care Med, 2015. **192**(3): p. 283-94.
8. Haura, E.B., et al., *Molecular origins of lung cancer: prospects for personalized prevention and therapy.* J Thorac Oncol, 2010. **5**(6 Suppl 3): p. S207-13.
9. Sacco, J.J. and M.J. Clague, *Dysregulation of the Met pathway in non-small cell lung cancer: implications for drug targeting and resistance.* Translational Lung Cancer Research, 2015. **4**(3): p. 242-252.
10. Webb, J.D. and M.C. Simon, *Novel insights into the molecular origins and treatment of lung cancer.* Cell Cycle, 2010. **9**(20): p. 4098-4105.
11. UyBico, S.J., et al., *Lung cancer staging essentials: the new TNM staging system and potential imaging pitfalls.* Radiographics, 2010. **30**(5): p. 1163-81.
12. Ruchalski, K.L. and K. Brown, *Lung Cancer Screening Update.* J Thorac Imaging, 2016. **31**(4): p. 190-200.
13. Gadgeel, S.M., S.S. Ramalingam, and G.P. Kalemkerian, *Treatment of lung cancer.* Radiol Clin North Am, 2012. **50**(5): p. 961-74.
14. Politi, K. and R.S. Herbst, *Lung Cancer in the Era of Precision Medicine.* Clinical Cancer Research, 2015. **21**(10): p. 2213-2220

15. Dhillon, S.S., et al., *Lung cancer screening update.* Journal of Carcinogenesis, 2013. **12**: p. 2.
16. Tanaka, K., K. Kumano, and H. Ueno, *Intracellular signals of lung cancer cells as possible therapeutic targets.* Cancer Science, 2015. **106**(5): p. 489-496.
17. Aggarwal, C., *Targeted therapy for lung cancer: present and future.* Annals of Palliative Medicine, 2014. **3**(3): p. 229-235.
18. Sangha, R., J. Price, and C.A. Butts, *Adjuvant Therapy in Non-Small Cell Lung Cancer: Current and Future Directions.* The Oncologist, 2010. **15**(8): p. 862-872.
19. Yasufuku, K. and T. Fujisawa, *Staging and diagnosis of non-small cell lung cancer: Invasive modalities.* Respirology, 2007. **12**(2): p. 173-183.
20. Liam, C.-K., et al., *Lung cancer staging now and in the future.* Respirology, 2015. **20**(4): p. 526-534.
21. Detterbeck, F.C., D.J. Boffa, and L.T. Tanoue, *The new lung cancer staging system.* Chest, 2009. **136**(1): p. 260-71.
22. Liam, C.K., et al., *Lung cancer staging now and in the future.* Respirology, 2015. **20**(4): p. 526-34.
23. Chang, A., *Chemotherapy, chemoresistance and the changing treatment landscape for NSCLC.* Lung Cancer, 2011. **71**(1): p. 3-10.
24. Schallier, D., et al., *A novel triplet regimen with paclitaxel, carboplatin and gemcitabine (PACCAGE) as induction chemotherapy for locally advanced unresectable non small cell lung cancer (NSCLC).* Lung Cancer, 2007. **56**(2): p. 247-54.
25. Rolfo, C., et al., *Improvement in lung cancer outcomes with targeted therapies: an update for family physicians.* J Am Board Fam Med, 2015. **28**(1): p. 124-33.
26. Lauro, S., et al., *The use of bevacizumab in non-small cell lung cancer: an update.* Anticancer Res, 2014. **34**(4): p. 1537-45.
27. Somasundaram A, B.T., *The next generation of immunotherapy: keeping lung cancer in check.*J Hematol Oncol., 2017. **10**(1): p. 87.
28. Wang, S.Q., et al., *Geridonin and paclitaxel act synergistically to inhibit the proliferation of gastric cancer cells through ROS-mediated regulation of the PTEN/PI3K/Akt pathway.* Oncotarget, 2016.
29. Rawat, D.S. and R. Singh, *Plant derived secondary metabolites as anti-cancer agents.* Anticancer Agents Med Chem, 2013. **13**(10): p. 1551.

30. Solowey, E., et al., *Evaluating medicinal plants for anticancer activity.* ScientificWorldJournal, 2014. **2014**: p. 721402.
31. Sultana, S., et al., *Medicinal plants combating against cancer--a green anticancer approach.* Asian Pac J Cancer Prev, 2014. **15**(11): p. 4385-94.
32. Gupta, R.C., et al., *Controlled-release systemic delivery - a new concept in cancer chemoprevention.* Carcinogenesis, 2012. **33**(8): p. 1608-15.
33. Aqil, F., et al., *Multi-layer polymeric implants for sustained release of chemopreventives.* Cancer Lett, 2012. **326**(1): p. 33-40.
34. Munagala, R., et al., *Bovine milk-derived exosomes for drug delivery.* Cancer Lett, 2016. **371**(1): p. 48-61.
35. Munagala, R., et al., *Withaferin A induces p53-dependent apoptosis by repression of HPV oncogenes and upregulation of tumor suppressor proteins in human cervical cancer cells.* Carcinogenesis, 2011. **32**(11): p. 1697-705.
36. Suman, S., et al., *Oral administration of withaferin A inhibits carcinogenesis of prostate in TRAMP model.* Oncotarget, 2016.
37. Hahm, E.-R. and S.V. Singh, *Withaferin A-induced apoptosis in human breast cancer cells is associated with suppression of inhibitor of apoptosis family protein expression.* Cancer Letters, 2013. **334**(1): p. 101-108.
38. Hahm, E.R., et al., *Withaferin A-induced apoptosis in human breast cancer cells is mediated by reactive oxygen species.* PLoS One, 2011. **6**(8): p. e23354.
39. Thaiparambil, J.T., et al., *Withaferin A inhibits breast cancer invasion and metastasis at sub-cytotoxic doses by inducing vimentin disassembly and serine 56 phosphorylation.* Int J Cancer, 2011. **129**(11): p. 2744-55.
40. Kakar, S.S., et al., *Withaferin a alone and in combination with cisplatin suppresses growth and metastasis of ovarian cancer by targeting putative cancer stem cells.* PLoS One, 2014. **9**(9): p. e107596.
41. Tong, X., H. Zhang, and B.N. Timmermann, *Chlorinated Withanolides from Withania somnifera.* Phytochem Lett, 2011. **4**(4): p. 411-414.
42. Mirjalili, M.H., et al., *Steroidal lactones from Withania somnifera, an ancient plant for novel medicine.* Molecules, 2009. **14**(7): p. 2373-93.
43. Samadi, A.K., *Potential Anticancer Properties and Mechanisms of Action of Withanolides.* Enzymes, 2015. **37**: p. 73-94.
44. Lee, I.C. and B.Y. Choi, *Withaferin-A-A Natural Anticancer Agent with Pleitropic Mechanisms of Action.* Int J Mol Sci, 2016. **17**(3).

45. Lavie, D., E. Glotter, and Y. Shvo, *1371. Constituents of Withania somnifera Dun. Part IV. The structure of withaferin A.* Journal of the Chemical Society (Resumed), 1965(0): p. 7517-7531.
46. Devi, P.U., *Withania somnifera Dunal (Ashwagandha): potential plant source of a promising drug for cancer chemotherapy and radiosensitization.* Indian J Exp Biol, 1996. **34**(10): p. 927-32.
47. Bharitkar, Y.P., et al., *Chemistry of withaferin-A: chemo, regio, and stereoselective synthesis of novel spiro-pyrrolizidino-oxindole adducts of withaferin-A via one-pot three-component [3+2] azomethine ylide cycloaddition and their cytotoxicity evaluation.* Mol Divers, 2015. **19**(2): p. 251-61.
48. Vanden Berghe, W., et al., *Molecular insight in the multifunctional activities of Withaferin A.* Biochem Pharmacol, 2012. **84**(10): p. 1282-91.
49. Bharitkar, Y.P., et al., *Chemistry of withaferin-A: chemo, regio, and stereoselective synthesis of novel spiro-pyrrolizidino-oxindole adducts of withaferin-A via one-pot three-component [3+2] azomethine ylide cycloaddition and their cytotoxicity evaluation.* Molecular Diversity, 2015. **19**(2): p. 251-261.
50. Fuska, J., et al., *Novel cytotoxic and antitumor agents. IV. Withaferin A: relation of its structure to the in vitro cytotoxic effects on P388 cells.* Neoplasma, 1984. **31**(1): p. 31-6.
51. Vyas, A.R. and S.V. Singh, *Molecular targets and mechanisms of cancer prevention and treatment by withaferin a, a naturally occurring steroidal lactone.* AAPS J, 2014. **16**(1): p. 1-10.
52. Patel, K., R.B. Singh, and D.K. Patel, *Pharmacological and analytical aspects of withaferin A: A concise report of current scientific literature.* Asian Pacific Journal of Reproduction, 2013. **2**(3): p. 238-243.
53. Misra, L., et al., *Selective reactivity of 2-mercaptoethanol with 5beta,6beta-epoxide in steroids from Withania somnifera.* Steroids, 2008. **73**(3): p. 245-51.
54. Mohan, R., et al., *Withaferin A is a potent inhibitor of angiogenesis.* Angiogenesis, 2004. **7**(2): p. 115-22.
55. Stan, S.D., et al., *Withaferin A causes FOXO3a- and Bim-dependent apoptosis and inhibits growth of human breast cancer cells in vivo.* Cancer Res, 2008. **68**(18): p. 7661-9.

56. Hahm, E.R., et al., *Metabolic alterations in mammary cancer prevention by withaferin A in a clinically relevant mouse model.* J Natl Cancer Inst, 2013. **105**(15): p. 1111-22.
57. Yang, H., G. Shi, and Q.P. Dou, *The tumor proteasome is a primary target for the natural anticancer compound Withaferin A isolated from "Indian winter cherry".* Mol Pharmacol, 2007. **71**(2): p. 426-37.
58. Kakar, S.S., V.R. Jala, and M.Y. Fong, *Synergistic cytotoxic action of cisplatin and withaferin A on ovarian cancer cell lines.* Biochem Biophys Res Commun, 2012. **423**(4): p. 819-25.
59. Kakar, S.S., et al., *DOXIL when combined with Withaferin A (WFA) targets ALDH1 positive cancer stem cells in ovarian cancer.* J Cancer Stem Cell Res, 2016. **4**.
60. Stockert, J.C., et al., *MTT assay for cell viability: Intracellular localization of the formazan product is in lipid droplets.* Acta Histochem, 2012. **114**(8): p. 785-96.
61. Rieger, A.M., et al., *Modified annexin V/propidium iodide apoptosis assay for accurate assessment of cell death.* J Vis Exp, 2011(50).
62. Wang, H., et al., *Resveratrol inhibits TGF-beta1-induced epithelial-to-mesenchymal transition and suppresses lung cancer invasion and metastasis.* Toxicology, 2013. **303**: p. 139-46.
63. Chou, T.-C., *Drug Combination Studies and Their Synergy Quantification Using the Chou-Talalay Method.* Cancer Research, 2010. **70**(2): p. 440.
64. Weaver, B.A., *How Taxol/paclitaxel kills cancer cells.* Mol Biol Cell, 2014. **25**(18): p. 2677-81.
65. Choi, B.Y. and B.-W. Kim, *Withaferin-A Inhibits Colon Cancer Cell Growth by Blocking STAT3 Transcriptional Activity.* Journal of Cancer Prevention, 2015. **20**(3): p. 185-192.
66. Nishikawa, Y., et al., *Withaferin A Induces Cell Death Selectively in Androgen-Independent Prostate Cancer Cells but Not in Normal Fibroblast Cells.* PLoS One, 2015. **10**(7): p. e0134137.
67. McKenna, M.K., et al., *Anti-cancer activity of withaferin A in B-cell lymphoma.* Cancer Biol Ther, 2015. **16**(7): p. 1088-98.
68. Cai, Y., et al., *Effect of Withaferin A on A549 cellular proliferation and apoptosis in non-small cell lung cancer.* Asian Pac J Cancer Prev, 2014. **15**(4): p. 1711-4.

69. Stepanenko, A.A. and V.V. Dmitrenko, *Pitfalls of the MTT assay: Direct and off-target effects of inhibitors can result in over/underestimation of cell viability.* Gene, 2015. **574**(2): p. 193-203.
70. Gonzalez, D.M. and D. Medici, *Signaling mechanisms of the epithelial-mesenchymal transition.* Sci Signal, 2014. **7**(344): p. re8.
71. Gemmill, R.M., et al., *ZEB1-responsive genes in non-small cell lung cancer.* Cancer Lett, 2011. **300**(1): p. 66-78.
72. Park, S.Y., et al., *Combinatorial TGF-beta attenuation with paclitaxel inhibits the epithelial-to-mesenchymal transition and breast cancer stem-like cells.* Oncotarget, 2015. **6**(35): p. 37526-43.
73. Valcourt, U., et al., *Analysis of Epithelial-Mesenchymal Transition Induced by Transforming Growth Factor beta.* Methods Mol Biol, 2016. **1344**: p. 147-81.
74. Liu, L.C., et al., *EGCG inhibits transforming growth factor-beta-mediated epithelial-to-mesenchymal transition via the inhibition of Smad2 and Erk1/2 signaling pathways in nonsmall cell lung cancer cells.* J Agric Food Chem, 2012. **60**(39): p. 9863-73.

LIST OF ABBREVIATIONS

ALK……Anaplastic Lymphoma Kinase

CI……..……..…..Combination Index

DMEM…….……Dulbecco's Modified Eagle Medium

DMSO…….Dimethyl Sulfo Oxide

EDTA……Ethylenediaminetetraacetic Acid

EGFR……..Epidermal Growth Factor Receptor

FBS……...……..Fetal Bovine Serum

FDA……..…….Food and Drug Administration

FITC……..……Fluorescein Isothiocyanate

HER2…….……Human Epidermal growth factor Receptor 2

LC……Lung Cancer

nM……..……...Nano Molar

NSCLC…….……...Non-Small Cell Lung Cancer

PAC…….…….Paclitaxel

PBS……..……..Phosphate Buffered Saline

PI……..Propidium Iodide

RPMI…….. Roswell Park Memorial Institute Medium

SD……...…….Standard Deviation

STAT3…….…..Signal Transducer and Activator of Transcription 3

TGFβ1……..Transforming Growth Factor beta 1

WFA…….……Withaferin A

WHO…….……..World Health Organization

μM…….Micro Molar

CURRICULUM VITAE

Al Hassan Kyakulaga

Department of Pharmacology and Toxicology
University of Louisville, School of Medicine
580 S. Preston Street, Rm. 319
Louisville, KY. 40202
502-654 237
alhassan.kyakulaga@louisville.edu / hkyakulaga@chs.mak.ac.ug

-

EDUCATION:

2005-2009: BBLT, Makerere University, Kampala, Uganda

2009-2012: MSc. Pharmacology, Makerere University, Kampala, Uganda

2014-Pres: Ph.D. Pharmacology & Toxicology, University of Louisville, Louisville, KY, U.S

ACADEMIC AND PROFESSIONAL APPOINTMENTS:

2008-2010: Research Assistant, Clinical Trial on developing a malaria prevention beverage. Uganda National Council for Science & Technology. Ministry of Science & Technology, Kampala, Uganda.

2009-2012: Teaching Assistant, Division of Pharmacology, Toxicology & Therapeutics, Makerere University, Kampala, Uganda.

2013-Pres: Assistant Lecturer (on study leave), Division of Pharmacology, b Toxicology & Therapeutics, Makerere University, Kampala, Uganda.

2014-Pres: Graduate fellow, Department of Pharmacology & Toxicology University of Louisville, Louisville, KY, USA

OTHER EMPLOYMENT:

2013-Pres: Lead scientist/consultant, development of antimalarial drugs for the Government of Uganda, DEI Natural Products International Kampala, Uganda.

2013-Pres: Co-founder & CEO, PKJ PharmaTOX Consultants (in partnership with Dr. Ogwang), Kampala, Uganda.

MEMBERSHIP IN PROFESSIONAL SOCIETIES:

2008-Pres: Uganda Society of Health Scientists (USHS)
2009-Pres: Makerere University Academic Staff Association (MUSA)
2013-Pres: Uganda Pharmacological Society (UPharS)
2014-Pres: American Society of Pharmacology & Experimental Therapeutics
2014-Pres: Society of Toxicology (SOT)

ACADEMIC AWARDS AND PROFESSIONAL HONORS:

2004: The best high school science student, 2004, M.M. College Wairaka, Uganda.
2005: The Government of Uganda Merit-Based Undergraduate Scholarship, 08/2005 – 08/2009.
2008: Undergraduate Research Scholarship, Natural Chemotherapeutics Research Laboratory, Ministry of Health, Kampala, Uganda, 08/2007-08/2008.
2009: Second Best Performing Undergraduate student, BLT Class 2009.
2011: Research Grant, Next Generation of African Academics, ($20,000), Carnegie Cooperation of New York, 08/2010-05/2012
2012: Recipient of outstanding Teaching Assistant, Makerere University Nominated by Students as best Pharmacology Instructor (2011/2012).
2012: Winner of the Trainee oral presentations award (2nd place), Natural Bio-actives Research Conference, London, Ontario, Canada (07/2012).
2013: Fulbright Science & Toxicology award, and Junior Staff Development award, selected as Principal Candidate from Uganda, 2012/2013.
2016: Best poster presenter award (1st place), (Biomedical sciences Master's student's category).Research Louisville! 2016

TEACHING EXPERIENCE:

Makerere University, Kampala, Uganda:

- BLT2102: General and systems pharmacology 2009-2014.
- BVM2104: Pharmacology, 2009-2014.
- BLT 2204: Toxicology, 2009-2014 (Course Coordinator/director)
- BM1103: General and Environmental Toxicology,
- BLT1202: Biomedical Instrumentation Principles,
- BLT1105: Principles of Quality Assurance & Control in Biomedical sciences.

University of Louisville, Louisville, KY, USA:

- DHED-402-01: Respiratory system pharmacology, Fall 2015
- BIOL-395-01: Basic Pharmacology, spring 2016.

SUPERVISION OF UNDERGRADUATE RESEARCH / DISSERTATIONS

1. **Mbabazi Angella** (2008). The acute toxicity effects of ethanolic extracts of *Bidens pilosa* and *Ocimu suave* in mice. Makerere University.
2. **Kibui Pauline** (2009). The analgesic and antiinflamatory activity of methanolic extracst of *Solanum incanum* in Rats. Makerere University.
3. **Miyingo Micheal** (2009): The Laxative activity of *Cassia dydbomotrya* in Rats. Makerere University.
4. **Biribawa Menya Victoria** (2010): The in vivo antihelmintic activity of ethanolic extracts of *Bidens pilosa* and *A. indica***.** Makerere University
5. **Alinda Thelma Brenda** (2010): The antidiarrheal activity of extracts of *Catharanthus Roseus* in Wistar albino rats**.** Makerere University.
6. **Mbuvi Christine** (2011). Antibacterial activity of aqueous extracts of *Psidium guajava* on multi-drug resistant strains of bacteria. Makerere University
7. **Mukiibi Karren** (2011): The antidiabetic activity of *Spathodea campanulata* in Wistar albino rats. Makerere University.
8. **Nanyonga Shamim** (2012). Antipyretic and analgesic activity of *Persea americana* in mice Makerere University.
9. **Kawalya Hakim**, (2012): The immunomodulatory effect of *B.pilosa* ethanolic extract in cyclophosphamide induced immunosuppression. Makerere University.
10. **Dhikusooka Ronald** (2013): Hepatoprotective activity of Solanum lycopersicum (tomato) in nevirapine induced hepatotoxicity in Wistar rats. Makerere University.

SELECTED PEER-REVIEWED ARTICLES:

1. Aqil, F., Kauser, H., Agrawal, A.K., Jeyaprakash, J., **Kyakulaga, A.H**., Munagala, R., and Gupta, R (2016). Exosomal formulation enhances the therapeutic response of celasterol against lung cancer. Experimental and Molecular Pathology. 101:12-21.
2. Radha, M., Aqil, F., Jeyabalan, J,. Agrawal, A.K., Mudd, A.M., **Kyakulaga, A.H**., Vadhanam, V.M., and Gupta, C.R (2017). Exosomal formulation of anthocyanidins against multiple cancer types. Cancer Letters. 94-102
3. Ogwang, P.E., Omujal, F., Agwaya, S.M., **Kyakulaga A.H**., and Obua, C (2015). Variations in antimalarial components of *Artemesia annua* Linn from three regions of Uganda. African Health Sciences. 15 (3): 828-834
4. **Kyakulaga. A.H,** C. Obua., Ogwang P.E., G Nakabonge and E.N Mwavu**:** Immunomodulatory effect of aqueous extracts of Auricularia sp and Pleurotus sp mushrooms on cyclophosphamide-induced immunosuppression in Wistar rats. British Journal of Pharmaceutical Research 3(4).
5. **Kyakulaga A.H**., Olia Deo and Ogwang P.E (2011). The wound healing potential of extracts of *Ocimum suave* and *Bidens pilosa* in Wistar rats. *African Journal of Pharmacy and Pharmacology* 5(2): 132-136
6. Ogwang P.E, Nyafuono J., Omujal F., Tumusiime R.H and **Kyakulaga A.H** (2011). Pre-clinical efficacy and safety of a herbal formulation for the management of wounds. *African Health Sciences*, 11(3): 524-529.
7. **Kyakulaga, A.H.**, Alinda, T.B., Vudriko, P. and Ogwang, P.E., (2011). *In vivo* antidiarrheal activity of the ethanolic extracts of *Catharanthus roseus* Linn in Wistar rats. African Journal of Pharmacy and Pharmacology. 5 (15): 1797-1800.

PROFESSIONAL REFEREES:

Dr. Ramesh Gupta, Ph.D.
Professor, Agnes Brown Duggan Chair of Oncological Research
Department of Pharmacology & Toxicology, University of Louisville,
580 S. Preston Street, 304E, 40202, Louisville, KY
Email: rcgupta@louisville.edu

Dr. Christopher States, Ph.D.
Professor, Vice-Chair for Graduate Education, Associate Dean for Research
Department of Pharmacology & Toxicology, University of Louisville,
505 S. Hancock Street, 304, 40202, Louisville, KY
Email: jcstates@louisville.edu

Dr. David Heine, Ph.D.
Professor and Chair, Pharmacology & Toxicology, University of Louisville,
505 S. Hancock Street, 305, 40202, Louisville, KY
Email: d.hein@louisville.edu

Dr. Francesca Aweeka, PharmD.
Professor & Director Drug Research Unit, School of Pharmacy, University of California, San Francisco, C-152, Box 0622, 521 Parnassus Avenue, San Francisco, CA 94143-0622. Phone: (415)-476-0339, Fax: (415)576-0307,
Email: faweeka@sfghsom.ucsf.edu

Dr. Jasper Ogwal Okeng, MBChB, MS, Ph.D.
Professor, Department of Pharmacology & Therapeutics
Makerere University, P.O. Box 7062 Kampala Uganda
Email: jogwal@chs.mak.ac.ug